Hierarchical Nanocomposites Derived from Nanocarbons and Layered Double Hydroxides - Properties, Synthesis, and Applications

Meng-Qiang Zhao, Qiang Zhang, Jia-Qi Huang, and Fei Wei**

The combination of one-dimensional and two-dimensional building blocks leads to the formation of hierarchical composites that can take full advantages of each kind of material, which is an effective way for the preparation of multifunctional materials with extraordinary properties. Among various building blocks, nanocarbons (e.g., carbon nanotubes and graphene) and layered double hydroxides (LDHs) are two of the most powerful materials that have been widely used in human life. This Feature Article presents a state-of-the-art review of hierarchical nanocomposites derived from nanocarbons and LDHs. The properties of nanocarbons, LDHs, as well as the combined nanocomposites, are described first. Then, efficient and effective fabrication methods for the hierarchical nanocomposites, including the reassembly of nanocarbons and LDHs, formation of LDHs on nanocarbons, and formation of nanocarbons on LDHs, are presented. The as-obtained nanocomposites derived form nanocarbons and LDHs exhibited excellent performance as multifunctional materials for their promising applications in energy storage, nanocomposites, catalysis, environmental protection, and drug delivery. The fabrication of LDH/carbon nanocomposites provides a novel method for the development of novel multifunctional nanocomposites based on the existing nanomaterials. However, knowledge of their assembly mechanism, robust and precise route for LDH/nanocarbon hybrid with well designed structure, and the relationship between structure, properties, and applications are still inadequate. A multidisciplinary approach from the scope of materials, physics, chemistry, engineering, and other application areas, is highly required for the development of this advanced functional composite materials.

1. Introduction

A good arrangement and construction of different low-dimensional nanomaterials (e.g., zero-dimensional (0D) nanoparticles (NPs), one-dimensional (1D) nanotubes, nanowires, nanorods, and two-dimensional (2D) flakes) as building blocks with two or more levels from the nanometer to the macroscopic scale leads to the formation of three-dimensional (3D) hierarchical nanocomposites. Hierarchical composites are widely observed in nature, e.g., in plant cell walls, bone, animal shells, and skeletons, showing that a high mechanical performance can be obtained by structuring matter across a range of length scales. The combination of low-dimensional nanomaterials with distinct physical and chemical properties into a composite with hierarchical structures can usually inherit full advantages of the component materials, or even lead to the formation of multifunctional materials with unexpected properties for unique applications. For instance, the combined clay/polymer,[1] carbon nanotube (CNT)/polymer,[2,3] or graphene/polymer[4] nanocomposites show significantly improved mechanical, electrical, and energy-absorbing properties. Clay/CNT nanocomposites obtained by growing CNTs on clays were demonstrated to be much more excellent nanofillers for polymer reinforcement[5] and were with better oil adsorption properties[6,7] compared with either clay or CNTs separately. They can even serve as an advanced material for shock-absorbing applications.[8] Tailored assembly of 1D CNTs and 2D graphene into 3D architectures can further explore the utilization and improve the performance of graphitic carbon materials in nanoelectronics, sensors, and energy storage/conversion devices.[9,10]

Exploring hierarchical composites with multifunctional properties through combining various building blocks together into a well-designed structure has always been a hot topic for material science. Among various building blocks, nanocarbons and layered double hydroxides (LDHs) were intensly investigated recently. On one hand, nanocarbon materials including fullerene, CNTs, and graphene, have been of great interest in the physics, chemistry, and materials communities since the first discovery of fullerene in 1985. Recently, the rapid progress of graphene and graphene-based materials has again triggered tremendous interest in 2D nanomaterials. On the other hand, LDHs are amongst the most studied advanced functional materials

M.-Q. Zhao, Prof. Q. Zhang, J.-Q Huang, Prof. F. Wei
Beijing Key Laboratory of Green Chemical Reaction Engineering and Technology,
Department of Chemical Engineering
Tsinghua University
Beijing 100084, P. R. China
E-mail: zhang-qiang@mails.tsinghua.edu.cn; wf-dce@tsinghua.edu.cn

DOI: 10.1002/adfm.201102222

and have been widely applied in the field of material science, catalysis, environment protection, biology, and energy in recent years. **Scheme 1** reveals the schematic structure of fullerene, CNT, graphene, and LDH. Fullerene resembles an association football of the type made of hexagonal and pentagonal carbon rings (Scheme 1a). According to their wall numbers, CNTs can be classified into single-walled CNTs (SWCNTs) and multi-walled CNTs (MWCNTs). The former one can be considered as a cylindrical tube formed by the wrapping of a single-layer graphene sheet (Scheme 1b). The latter one can be considered as an array of such nanotubes that are concentrically nested. Graphene, a 2D monolayer sheet of sp^2 hybridized carbon atoms (Scheme 1c), is believed to be the basic building block of various carbon allotropes. It is also an excellent building block for 3D hierarchical nanocomposites. LDHs have been known for more than 150 years since the discovery of the mineral hydrotalcite, and their main structure was understood by single X-ray diffraction investigation.[11] Also known as hydrotalcite-like materials, LDHs are a class of synthetic 2D nanostructured anionic clays, whose structure is based on brucite ($Mg(OH)_2$)-like layers (Scheme 1d). The general formula of LDHs can be represented as $M^{2+}_{1-x}M^{3+}_x(OH)_2A^{n-}_{x/n}\cdot mH_2O$, where M^{2+} and M^{3+} are di- and trivalent metal cations, respectively; x is defined as the molar ratio of $M^{3+}/(M^{2+}+M^{3+})$ and generally has a value ranging from 0.2 to 0.33; A^{n-} are the interlayer anions.[11] The nanocarbons and LDHs exhibit unique but distinguishing physical and chemical properties, which are complementary to a certain extent. Therefore, many efforts have been devoted on the exploration of hierarchical nanocomposites with improved or extended properties from the combination of nanocarbon materials and LDHs based on their synergic effect.[12–14]

This Feature Article highlights the recent research progress and achievements on the hierarchical nanocomposites derived from nanocarbon and LDH materials. In the second part, the property of nanocarbons, LDHs, and their composites are briefly summarized. Then the synthesis routes are illustrated to give the basic materials chemistry for the fabrication of the hierarchical nanocomposites. The applications of the nanocomposites in the area of energy, materials science, catalysis, environments, and biology are introduced. Current challenges and future strategies are discussed.

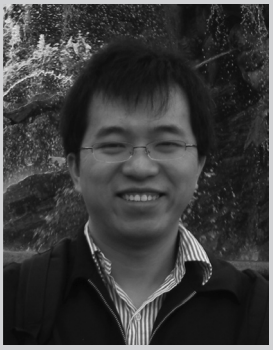

Qiang Zhang graduated from the Chemical Engineering Department, Tsinghua University, P. R. China, in 2004, where he continued doing research on mass production of carbon nanotubes and obtained his PhD in chemical engineering in 2009. After a short stay as a Research Associate in Case Western Reserve University, USA, in 2009, he joined the Fritz Haber Institute of the Max Planck Society, Germany, as a post-doctoral fellow. He was appointed Associate Professor of chemical engineering of Tsinghua University in 2011. His current research interests are nanocarbon, advanced functional materials, sustainable chemical engineering, energy conversion, and storage.

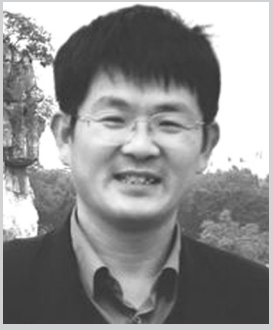

Fei Wei obtained his PhD in chemical engineering from China University of Petroleum in 1990. After a postdoctoral fellowship at Tsinghua University, he was appointed Associate Professor in 1992 and Professor of chemical engineering at Tsinghua University in 1996. He was also a Visiting Professor at Ohio State University, USA, University of Western Ontario, Canada, and Nagoya Institute of Science and Technology, Japan. He is now Director of the Fluidization Laboratory of Tsinghua University (FLOTU). His scientific interests are chemical reaction engineering, multiphase flow, advanced materials, and sustainable energy.

2. Properties of LDHs, Nanocarbons, and their Derived Composites

2.1. Properties of Nanocarbons

Nanocarbons, such as 0D fullerenes, 1D CNTs, and 2D graphene, are materials with excellent physical and chemical properties owing to their low-dimensional structure and sp^2 hybridization of carbon atoms, as summarized in **Table 1**. For instance, CNTs exhibit excellent mechanical properties with Young's moduli of 0.27–1.25 TPa[15,16] and a tensile strength of 11–63 GPa,[16,17] which make them high-performance nanofillers for nanocomposites.[2] CNTs also show a low band gap of 0–1.9 eV,[18] high electrical conductivity of $0.17–2\times10^5$ S cm^{-1},[19] and high thermal conductivity of 3000–6600 W m^{-1} K^{-1}.[20] The excellent electrical and thermal properties of CNTs facilitate their applications in the field of electrical devices, energy conversion and storage,

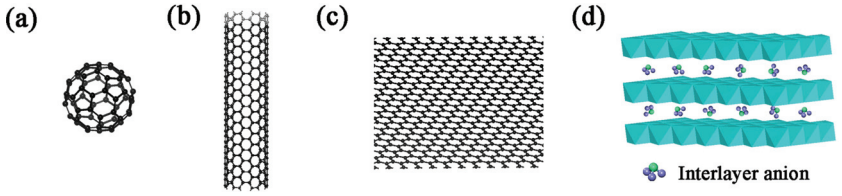

Scheme 1. Schematic illustration showing the structures of a fullerene (a), a CNT (b), graphene (c), and LDH (d).

Table 1. Properties of nanocarbons and LDHs.

Properties	Fullerenes	CNTs	Graphene	LDHs
Young's modulus [GPa]	15.9[32]	0.27–1.25[15,16]	~1.0[25]	/
Tensile strength [GPa]	/	11–63[16,17]	130[25]	/
Band gap [eV]	1.5–2.0[33]	0–1.9[18]	0[24]	/
Electrical conductivity [S cm^{-1}]	10^{-14}–6×10^{-8}[33,34]	0.17–2×10^{5}[19]	~10^{6}[26]	unconductive
Thermal conductivity [W m^{-1} K^{-1}]	0.4[35]	3000–6600[20]	3000–5000[27]	/
Specific surface area [m^2 g^{-1}]	/	150–1315[22]	2630[24]	20–120[36]
Chemical reactivity	Inert	Inert	Inert	Active

transparent conductive films, field emission displays, thermal interface materials, etc.[21] Besides, the high specific surface area (150–1315 m^2 g^{-1})[22] and good thermal stability of CNTs[23] triggered the researches about using CNTs as catalyst supports. As a kind of one-atomic graphitic carbon layer, graphene has attracted extensive attentions since its discovery.[24] It also has excellent mechanical, electrical, and thermal properties, such as a large theoretical specific surface area (2630 m^2 g^{-1}),[24] high Young's modulus (~1.0 TPa) and tensile strength (130 GPa),[25] much lower band gap (0 eV),[24] high electrical (~10^6 S cm^{-1})[26] and thermal conductivity (3000–5000 Wm $^{-1}$ K^{-1}).[27] These properties stimulated the investigations on applying graphene in the field of electronic and energy devices, transparent conductive films, polymer nanocomposites, etc.[28]

Due to the chemical inertness of carbon atoms, nanocarbons show a lack of chemical reactivity. However, defects exist on the surface or at the edge of nanocarbons, such as CNTs and graphene, which are easy to be oxidized and functionalized.[9,28–30] The functionalization of CNTs or graphene either by covalent or noncovalent methods decorate these nanocarbons with functional groups, which not only improve the solubility of these nanocarbons, but also gives rise to their chemical reactivity. Besides, some heterogeneous elements, such as N and B, can be doped into the lattice of the graphitic nanocarbons, which changes their band gap and improves their chemical reactivity.[31] Functionalized CNTs and graphene have been widely investigated as great candidates for high-performance nanocomposites, catalyst, adsorption, drug delivery, etc.[4,21,28,30]

2.2. Properties of LDHs

Most metals, such as Mg, Al, Fe, Co, Ni, Cu, Zn, etc., can be dispersed on the atomic level in a lamellar LDH flake with controllable components. The substitution of divalent metal cations with trivalent cations leads to positively charged LDH layers, which are charge balanced by a wide variety of anions within their interlayer domains.[11] LDHs are usually composed of hexagonal flakes with a lateral size of tens of nanometers to several micrometers and a thickness of tens of nanometers. The specific surface area of as-obtained LDHs is ranging from 20 to 120 m^2 g^{-1}.[36] As a kind of 2D anionic clay, LDHs exhibit excellent performance on the polymer reinforcement as nanofillers.[37] Due to most kinds of metals can be well dispersed into the LDH layers in an ordered/well-defined arrangement, LDHs also play an important role in the field of heterogeneous catalysis.[38,39] Calcination of LDHs leads to the formation of layered double oxides (LDOs) with mixed metal oxides or spinels as the main component. The LDOs also act as good catalysts for various chemical reactions.[38] Besides, due to the strong interaction between LDHs and the arranged metals, LDHs are widely explored as catalyst support.[40] Certain kind of LDHs, such as CoAl and NiAl LDHs, show a high activity for the faradic redox reaction, which facilitates their use for energy conversion and storage, such as electrode materials for supercapacitor.[41] Some of the possible compositions for unitary and binary LDHs are presented in **Table 2**. The colored cells reveal the possible association of metallic cations for the LDHs, among which the blue cells indicate the associated LDHs are with catalytic activity for nanocarbon growth.

One of the most important properties for LDHs is their excellent anion-exchange ability. Almost all kind of anions, including anionic inorganic micromoleculars and organic macromoleculars, can be intercalated into the interlayer space of LDHs through co-precipitation or anion-exchange process.[11] The calcination of LDHs at high temperatures always results in the loss of their interlayer anions and destroys their hydrotalcite-like structure. However, when the as-obtained LDOs are immersed in anionic solutions, they exhibited a strong tendency to reconstruct their hydrotalcite-like structure, accompanied with the high intercalation capacity of the anions.[42] This triggered studies to use LDHs and LDOs for adsorption, storage and release of functional anions.[43] The interlayer anions also play an important role in the properties of LDHs. For instance, when organic anions with optical properties were intercalated into the interlayer space of LDHs, the as-obtained LDHs can be applied as good optical materials.[44] Furthermore, when LDHs were dispersed into polar solutions, such as formamide, the intercalation of the polar monomer can lead to the delamination of LDH flakes into single-layer LDH nanosheets. As another kind of one-atomic-thick material, single-layer LDHs can further extend the utilities of LDHs.[45]

2.3. Properties of the LDH(LDO)/Carbon Nanocomposites

As mentioned above, nanocarbons and LDHs are all exciting materials with excellent properties. However, their applications are still limited due to their intrinsic shortages. For instance, the electrochemical performance of LDHs is seriously hindered by their low electrical conductivity though they are

Table 2. Potential compositions of LDHs: The colored cells reveal the possible association of metallic cations for the LDHs, among which the blue cells indicate the associated LDHs are with catalytic activity for nanocarbon growth.

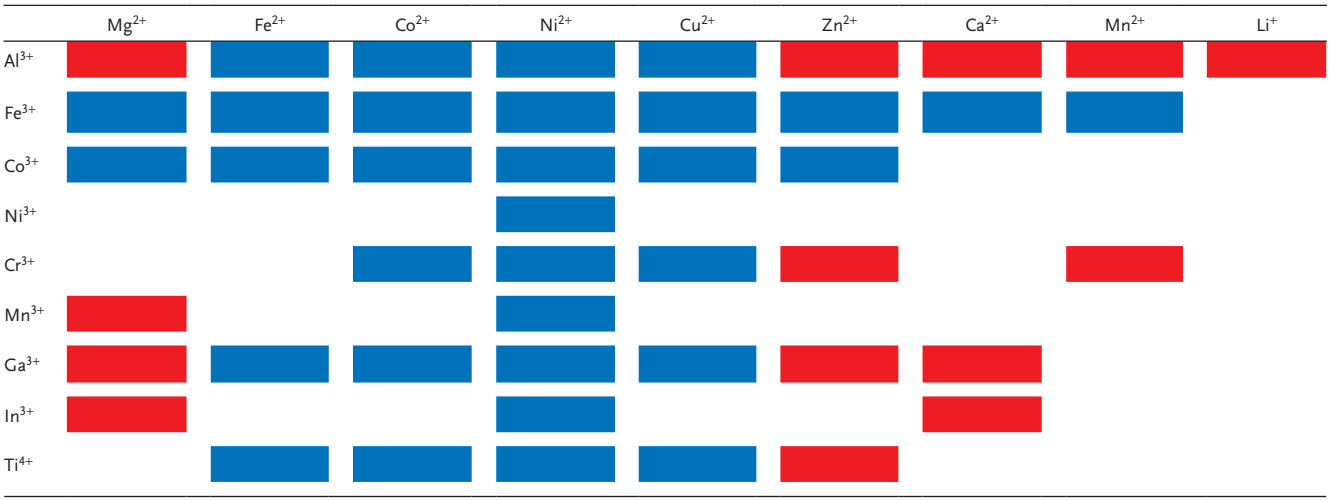

with high chemical reactivity. And for nanocarbons with high electrical conductivity, such as CNTs and graphene, the electrochemical performance is mainly hindered by their chemical inertness.[46,47] Besides, the intercalation properties for LDHs are mainly corresponding to anionic molecules, while the original and functionalized CNTs show strong interaction with neutral and cationic molecules. In addition, as nanomaterials, both nanocarbons and LDHs encounter the problems of aggregation during their application. It should be noticed that most of the properties of nanocarbons and LDHs are complementary. Therefore, the combination of nanocarbons and LDHs into hierarchical nanocomposites is a promising method to integrate their distinguishing properties together: nanocarbons can provide the good electrical conductivity and high mechanical strength, and LDHs can provide good chemical reactivity. Thus, an electron pathway can be easily formed and a network of stress transfer can be also presented between the nanocarbons and LDHs, which is an important aspect as advanced functional materials. In another aspect, such structured nanocomposites are always with a porous structure. When they were employed as catalyst, the heat and mass transfers during a reaction can be greatly improved (nanocarbons were with a high thermal conductivity) and more active sites can be easily exposed to the reactant, which is helpful for the high rate conversion of the reactants. In some case, the as-obtained well-designed structure also presents unexpected property, such as unique porous structures for ion, molecular diffusion behavior modulation, and tailored micro-, meso- together with an appropriate macroporosity for catalysis and energy conversion and storage.

3. Synthesis of LDH(LDO)/Carbon Nanocomposites

Controllable synthesis of LDH(LDO)/nanocarbon hierarchical composites is the first step to explore their fascinating properties and broad applications. Many types of hierarchical LDH(LDO)/carbon nanocomposites derived from LDHs and fullerene (**Scheme 2**A), CNTs/CNFs (Scheme 2B), graphene (Scheme 2C), as well as mesoporous carbons could be fabricated to achieve a synergic combination of nanocarbons and LDHs.

Due to the complex interactions between nanocarbons and LDHs, the fabrication of the combined nanocomposite is just like an art to build 3D nanoarchitectures. The number of studies exploring a way of manipulating the interactions between nanocarbons and LDHs by materials chemistry and physics for the fabrication of LDH(LDO)/carbon nanocomposites is increasing On one hand, based on the strong electrostatic force between the positively charged surface of LDHs and the negatively charged surface of nanocarbons, reassembly of nanocarbons and LDHs is one of the most frequently used methods for the fabrication of LDH/carbon nanocomposites. On the other hand, if LDHs(LDOs) or nanocarbons were employed as the growth substrates, the other phase can be formed in situ on the substrates. For instance, the synthesis of LDHs always corresponds to a process of the coprecipitation of metal cations and the following crystal growth in solutions; thus, the fact that the negatively charged surface of nanocarbons exhibits strong adsorption ability for the metal cations in solution makes nanocarbons suitable supports for in situ growth of various kinds of LDHs due to their large specific surface area. Furthermore, since various organic anions can be easily intercalated into the interlayer space of LDHs, the carbonization of these interlayer anions can lead to the formation of LDO/carbon nanocomposites. In addition, LDHs with transition metals can be widely used as catalysts for the in situ growth of nanocarbons, and LDO/carbon nanocomposites with various kinds of hierarchical structures can be fabricated. In this section, we tried to briefly summarize the efficient and effective routes for the fabrication of LDH(LDO)/carbon nanocomposites by the reassembly of nanocarbons and LDHs, direct formation of LDHs on nanocarbons, and direct formation of nanocarbons on LDHs by carbonization or chemical vapor deposition (CVD).

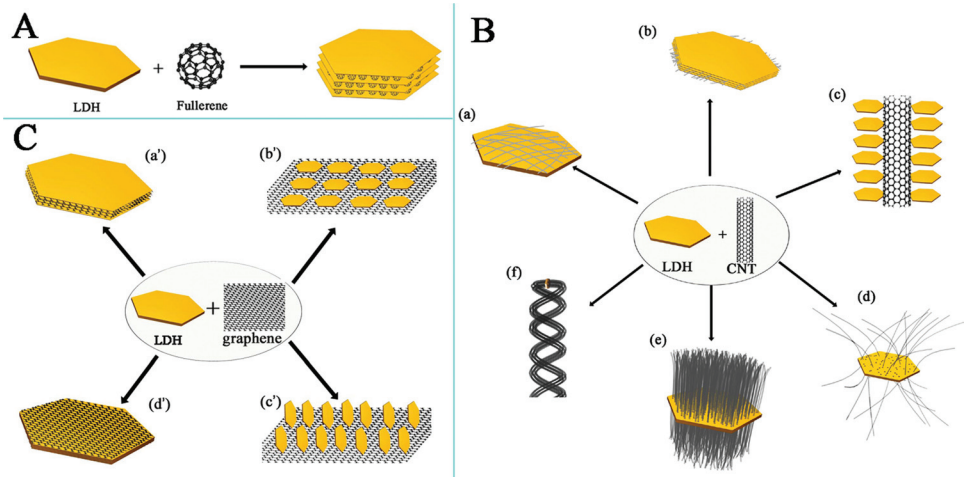

Scheme 2. Schematic illustration showing: A) the possible structures of C_{60}+LDH:C_{60} intercalated into the interlayer spaces of LDHs; B) CNT+LDH: a) CNTs uniformly attached on the surface of LDH flakes; b) intercalation of CNTs into the interlayer space of LDHs; c) LDHs in situ grown on the surface of CNTs; d) randomly entangled CNTs grown from LDHs; e) aligned CNT arrays grown from LDHs; f) CNT-array double helix grown form LDHs; and C) Graphene+LDH: a') intercalation of graphene layers into the interlayer space of LDHs; b') in situ grown LDHs parallel to the graphene layer; c') in situ grown LDHs vertically to the graphene layer; d') graphene in situ grown on the surface of LDHs.

3.1. Reassembly of Nanocarbons and LDHs

3.1.1. Directly Mixing LDHs and Nanocarbons

The simplest method to fabricate LDH/carbon nanocomposites is to directly mix the nanocarbon material with an LDH dispersion. By mixing dodecyl sulfate intercalated MgAl LDH powders with toluene or hexane solutions of C_{60}, the C_{60} molecules can be dissolved into the interlayer hydrophobic phase of LDHs. The decomposition of dodecyl sulfate anions by heating the resultant compound under vacuum led to the formation of LDH/C_{60} nanocomposites with C_{60} molecules sandwiched between the LDH layers (Scheme 2A).[48] Besides, when the positively charged LDHs were mixed with negatively charged nanocarbons, the strong interaction attributed from electrostatic interaction leads to their reassembly into LDH/carbon nanocomposites directly. When functionalized CNTs and LDHs were mixed ultrasonically in water,[47,49] the negatively charged surface of the functionalized CNTs attributed from the existence of carboxyl groups exhibited strong interaction with the LDH flakes, leading to the formation of LDH/CNT nanocomposites with MWCNTs adhering to the surface of LDH flakes (**Figure 1**A). It should be noticed that LDHs can be easily delaminated to form single-layer nanosheets by using micrometer-sized hexagonal LDH flakes as a precursor and formamide as a delaminating reagent.[50] The delamination of LDHs allows to further explore the utility of LDHs, since single-layer LDHs usually have a diameter of about several micrometers and a thickness below 1 nm and shows a high aspect ratio of about 1000 or more. Therefore, exfoliated LDH/carbon nanocomposites are of high interest. For example, when the CoAl LDH flakes was dispersed into formamide by stirring, a colloidal suspension of single-layer LDH nanosheets can be formed. When mixed with CNT-COONa solution, the colloidal suspension was broken down, and the single-layer LDHs and CNTs coprecipitated in the formamide after the introduction of CNTs.[51] Exfoliated LDH/CNT nanocomposites with CNTs randomly distributed on the surface of single-layer LDHs were obtained through this coassembling process of positively charged single-layer LDH nanosheets with negatively charged CNTs, as shown in Figure 1B. A similar phenomenon was also observed when a carboxylated graphene oxide (GO) dispersion was added into the LDH colloidal suspension.[52] The strong electrostatic force between the single-layer LDHs and GO facilitated the layered assembling of the two one-atom-thick sheets, and the as-obtained exfoliated LDH/GO nanocomposites exhibited an ordered layer structure (Figure 1C).

Directly mixing is a facile and economic method to obtain LDH/nanocarbon nanocomposites on a large scale. However, it is still a great challenge to obtain well-designed architectures with homogenous structures for the reason that the interaction between nanocarbons and LDHs is too complex. Finding a dominated interaction between nanocarbons and LDHs to manipulate their self assembly is quite necessary.

3.1.2. Layer-by-Layer Self-Assembly

Self-assembly is a process that occurs due to the spontaneous and uninstructed structural reorganization that forms from a disordered system. The layer-by-layer (LBL) self-assembly technique has emerged as a versatile and convenient method for the construction of ultrathin multilayer hybrid films due to their well-defined architecture at the nanometer scale and well-controlled chemical composition.[53] Both LDHs[54] and nanocarbons[55] have been demonstrated to be LBL self-assembled with other kind of materials. Recently, Chen et al.[56] reported the fabrication of multilayer LDH/graphene composites by utilizing the hydrogen-bonding LBL self-assembly method. Quartz glass slides, cleaned by treatment in a bath of H_2SO_4/H_2O_2 and then thoroughly rinsed with deionized water and dried under nitrogen flow, were used as the substrate. The substrate was

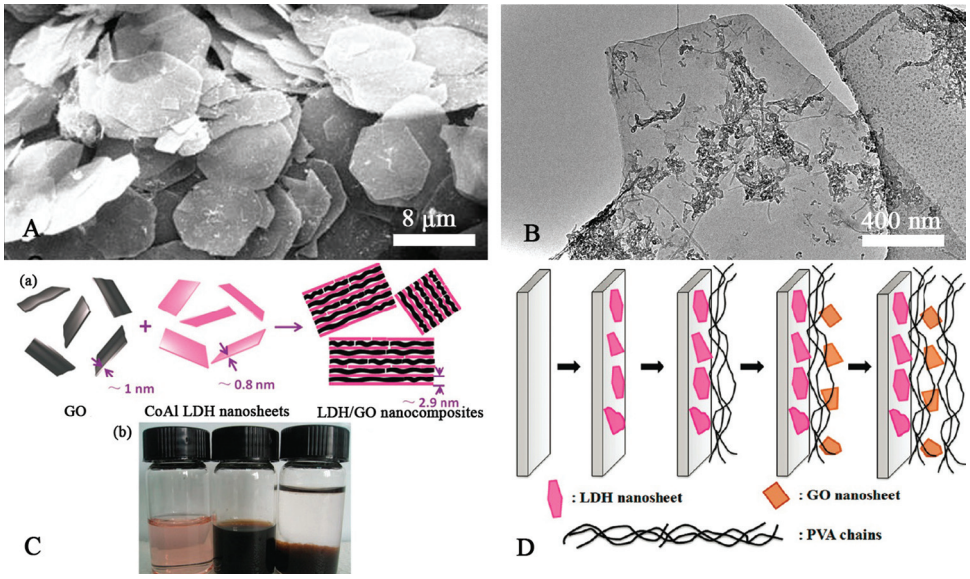

Figure 1. Reassembly of nanocarbons and LDHs: A) Scanning electron microscopy (SEM) image of CoAl LDH/CNT nanocomposites. Reproduced with permission.[49] Copyright 2008. Springer. B) Transmission electron microscopy (TEM) image of single-layer CoAl LDH/CNT nanocomposites obtained by direct mixing. Reproduced with permission.[51] Copyright 2010, American Chemical Society. C) LDH/GO nanocomposites obtained by direct mixing: a) schematic illustration of the formation of CoAl LDH/GO nanocomposites, b) digital photographs of the aqueous dispersion of (left) single-layer CoAl LDHs, (middle) GO, and (right) a mixture of single-layer CoAl LDHs and GO. Reproduced with permission.[52] Copyright 2011, Royal Society of Chemistry. D) Schematic illustration of the formation of LDH/GO nanocomposites by layer-by-layer self-assembly. Reproduced with permission.[56] Copyright 2010, American Chemical Society.

cyclically dipped into the solution of exfoliated LDHs, poly(vinyl alcohol) (PVA), exfoliated GO, and PVA, with each step followed by water washing and nitrogen drying (Figure 1D). By a simple and effective *in situ* reduction process, multilayer nanocomposites films containing monolayer dispersed LDHs and graphene can be obtained.

The LDH/carbon nanocomposites obtained by the reassembly of LDHs and nanocarbon materials can well retain the original structure of LDHs or exfoliated LDHs and nanocarbon materials and thus can fully inherit the intrinsic properties of both the LDHs and nanocarbons. In most cases, only electrostatic force was adopted for the reassemble process and the structure of the as-obtained nanocomposites is thus limited, which hinders further applications of the LDH/carbon nanocomposites. However, with the assistance of other kind of materials, other driving forces, such as hydrophobic interaction and hydrogen bonding, can also be adopted for the reassembly of nanocarbons and LDHs, which is a promising method to extend the structure style of the LDH/carbon nanocomposites.

3.2. Direct LDH Formation on Nanocarbons

The most commonly used method for the preparation of LDHs is coprecipitation of the chosen divalent and trivalent cations from solution.[57] When materials with certain adsorption capacity of the cations were added into the solution during the coprecipitation process, precipitation will occur on the surface of these materials, leading to the in situ growth of LDHs. Hsieh et al.[58] fabricated LDH/carbon fiber (CF) composites by immersing carbon cloth in an aqueous alkaline Al^{3+}– and Li^{+}–containing solution at room temperature (**Figure 2**a). Highly oriented LiAl LDH films were obtained on both the hydrophobic and hydrophilic carbon cloth surfaces, and the LDH film thickness increased with immersion time and/or solution temperature.

Functionalized nanocarbon materials, such as carbon nanofibers (CNFs) or CNTs, can also be used as the substrates for the in situ growth of LDHs. For instance, when CNFs were treated in concentrated nitric acid, a large amount of oxygen-containing groups (e.g., hydroxyl and carboxyl groups) can be introduced. The functionalized CNFs were first impregnated with an aqueous solution containing both $Mg(NO_3)_2$ and $Al(NO_3)_3$ to adsorb Mg^{2+} and Al^{3+}. After drying, the material was impregnated with another aqueous solution containing both NaOH and Na_2CO_3 for coprecipitation; hydrothermal treatment was carried out on the impregnated samples subsequently for crystal growth, and MgAl LDH loadings as high as 16% were obtained.[59] The LDHs turned out to be presented as platelets with a lateral size of ca. 20 nm supported on the CNFs. A NiAl LDH/CNT nanocomposite can be synthesized through a similar procedure.[60] Compared with pure NiAl LDHs, the interlayer distance for LDHs in the composites became slightly larger, suggesting that the precipitation of LDH crystallites on CNTs probably involved the formation of interactions between LDH and the CNT surfaces. The mass ratio of LDHs in the as-prepared LDH/CNT nanocomposites was controllable and can be as high as 79.3%. The surface coverage of LDH particles with a lateral size of 10–15 nm in composites decreased progressively with the decreasing mass ratio of LDHs to CNTs. Besides, the

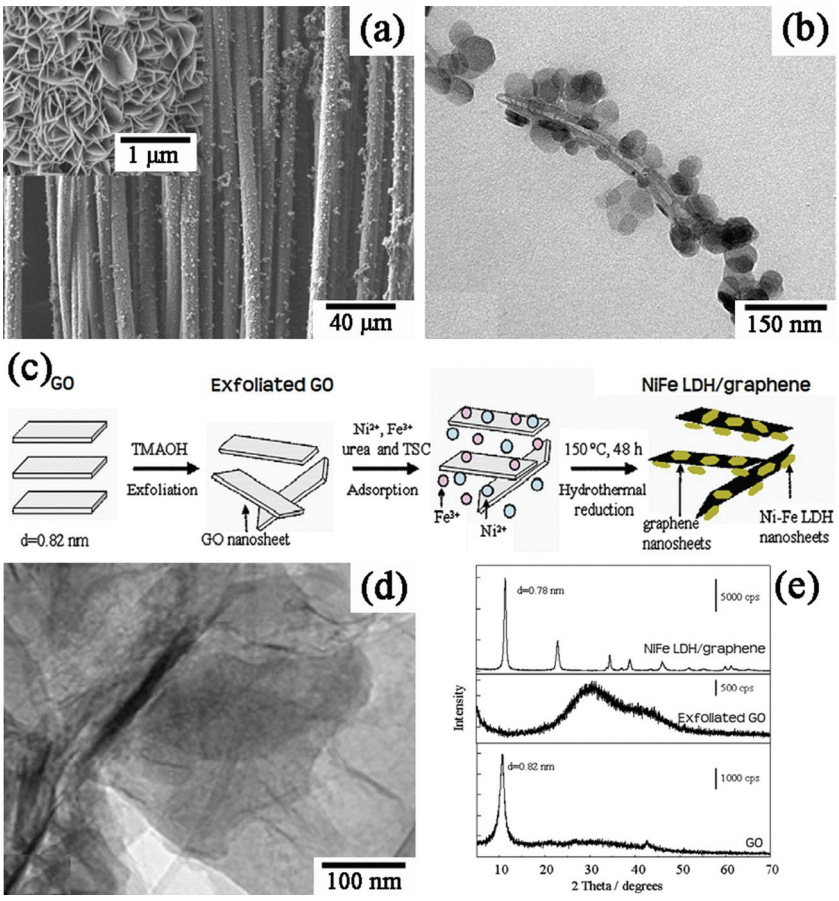

Figure 2. Growth of LDHs on nanocarbons**:** a) SEM image of LiAl LDHs grown on carbon fibers. Reproduced with permission.[58] Copyright 2011, Royal Society of Chemistry; b) TEM image of NiAl LDHs grown on MWCNTs. Reproduced with permission.[14] Copyright 2011, IOP Publishing; c) Schematic of the formation process of NiFe LDH/graphene nanocomposites from in situ growth of LDHs on graphene layers. d) TEM image of NiFe LDH flake (the hexagonal particle) grown on graphene; e) XRD patterns of the precursor GO, exfoliated GO and the as-grown NiFe LDH/graphene nanocomposites. Reproduced with permission.[12] Copyright 2010, Elsevier.

functionalization degree of CNTs also played an important role in the surface coverage of LDHs.[14] The size of the LDH particles can be controlled by the temperature and the hydrothermal reaction duration. CNTs wrapped by NiAl LDHs with a size of 30–100 nm were prepared with the hydrothermal reaction at 100 °C for 24 h (Figure 2b).[14] 2D GO was also found to be an effective substrate for the in situ growth of LDHs.[12,61] By dispersing delaminated GO into a mixture of $Ni(NO_3)_2$, $Fe(NO_3)_3$, urea, and trisodium citrate followed by hydrothermal treatment, LDH/graphene nanocomposites of NiFe LDH particles with a mean lateral size of 350 nm homogeneously grown on the surface of graphene nanosheets were prepared (Figure 2c–e). The GO nanosheets were simultaneously reduced into graphene during the coprecipitation of the LDHs.[12] NiAl LDH/graphene nanocomposites were also fabricated by a similar process.[61] During the in situ growth of LDHs on the functionalized nanocarbon materials, the functional groups give rise to the negatively charged surface of these materials, which exhibit strong electrostatic force with the cations in the solution, and lead to the precipitation of LDHs on the surface of the nanocarbon materials.

The in situ growth of LDHs on the surface of nanocarbon materials gives rise to the strong interaction between the positively charged LDH flakes and the negatively charged carbon materials. The as-obtained LDH/carbon nanocomposites also can well retain both the intrinsic structures and properties of the LDHs and carbon materials. This provides another effective method for the combination of the two kinds of material. However, for the growth of LDHs on nanocarbon materials, the size of LDH flakes is always limited due to the nanometric size of the substrate, which may hinder their further applications.

3.3. Direct Nanocarbon Formation on LDHs

3.3.1. Carbonization of interlayer anions of LDHs

One of the main advantages of LDHs is their unusual anion intercalation property. Various anions can be intercalated into the interlayers of LDHs, which makes the LDHs to "nanoreactors" and extends the application fields of LDHs as supported catalysts,[62] multifunctional materials,[63] and compatible inorganic fillers.[64] In particular, organic anions, including polymer macromolecules, can also be intercalated into the interlayer space of LDHs. Carbonization under inert conditions of these interlayer anions can give access to a variety of interesting carbonaceous nanocomposites. This provides another effective method for the fabrication of hierarchical nanocomposites based on LDHs and nanocarbon materials.

Anion exchange and direct coprecipitation are two of the mainly used processes for the intercalation of organic anions into LDH interlayer spaces. Early in 1995, Putyera et al.[65] calcined MgAl-CO_3 LDHs at 450 °C for 3.0 h to remove the CO_3^{2-} anion. Then the calcined MgAl-CO_3 LDHs were treated with a solution of styrene(4-sulfonate) anion under an inert atmosphere to obtain 4-styrenesulfonate anion-intercalated MgAl LDHs by structural regeneration. After subsequent in situ polymerization, the as-obtained LDH/poly(4-styrenesulfonate) was heat treated in a flow of nitrogen at 600 °C for 3.0 h to induce the carbonization of the interlayer poly(4-styrenesulfonate). The carbonization process performed at high temperature induced the decarboxylation and dehydroxylation of LDHs and led to the formation of LDOs. It was found that the carbonization between the layers of LDHs gave rise to the formation of highly microporous carbons without additional activation process. As a result, hierarchical nanocomposites composed of LDOs and mesoporous carbons were obtained.

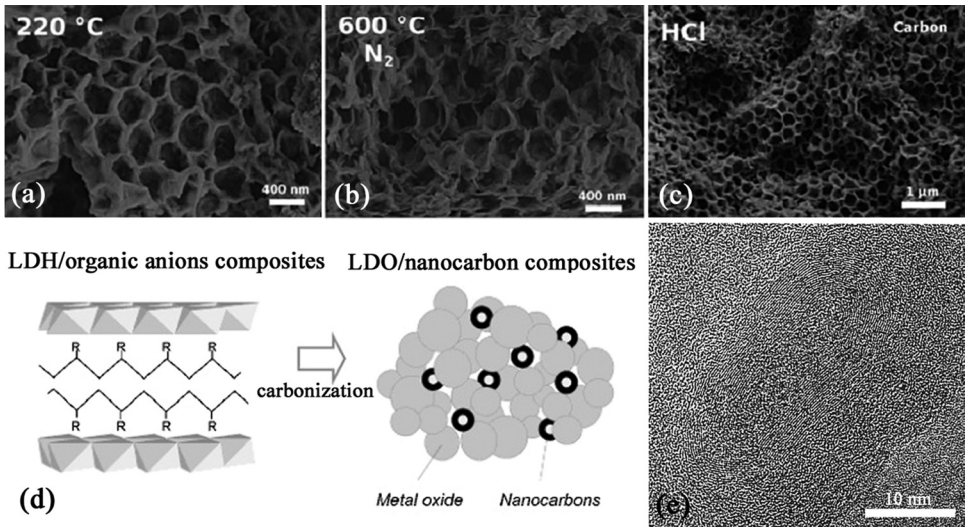

Figure 3. Carbonization of the interlayer anions of LDHs: SEM images of a) 3-DOM MgAl LDH/VBS composites, b) 3-DOM LDO/porous carbon nanocomposites after carbonization under N_2 atmosphere, and c) the corresponding 3-DOM meso-porous carbon after acid-leaching step. Reproduced with permission.[70] Copyright 2010, Royal Society of Chemistry. d) Schematic illustration of LDO/CNP nanocomposites obtained by the carbonization of organic anions intercalated and transition metal-containing LDHs. Reproduced with permission.[73] Copyright 2001, American Chemical Society. e) High-resolution TEM images showing the CNPs obtained from the carbonization of TA^{2-} intercalated CoMgAl LDHs. Reproduced with permission.[72] Copyright 2000, American Chemical Society.

Similar result was also reported with 1,5-naphthalene disulfonate dianion as the intercalated organic anion.[66] Hibino et al.[67] directly precipitated MgAl LDHs in an organic anion solution (malonate, glutarate, pimelate, and phthalate) to prepare organic anion-intercalated LDHs. LDO/mesoporous-carbon nanocomposites were also obtained after the carbonization of the interlayer anions. Recently, Leroux and Dubois reported a series of excellent progresses on the fabrication of LDO/mesoporous carbon nanocomposites through the carbonization of the interlayer anions of LDHs. Various kinds of organic anions, such as poly(vinylbenzene-4-sulfonate) (VBS),[68] poly(styrene sulfonate),[69] 3-sulfopropylmethacrylic acid[70] and 2-acrylamido-2-methyl-1-propanesulfonate acid,[71] were all demonstrated to be effective interlayer anions for carbonization. Especially, a 3D ordered macroporous (3-DOM) LDO/mesoporous carbon nanocomposite was also fabricated.[70] MgAl LDH coprecipitation was conducted around the 3D ordered polystyrene beads to form a 3-DOM LDH structure. VBS monomer was intercalated into the interlayer of such 3-DOM LDHs through anion exchange by calcination and a subsequent regeneration process. Successive steps of VBS in situ polymerization and carbonization were conducted to yield to the 3-DOM LDO/mesoporous carbon nanocomposites (**Figure 3**a and b). When acid-etching is carried out on the above-mentioned LDO/carbon nanocomposites to remove the LDOs, porous carbon with a large quantity of micro/mesoporous structures can be obtained that are of promising properties for applications (Figure 3c).

The existence of transition metal, such as cobalt, in the cation layer can induce graphitization of carbon in the LDO/carbon composites during the carbonization process to form graphitic carbon nanomaterials (Figure 3d). For instance, a LDO/carbon nanoparticles (CNPs) composite can be easily fabricated through the carbonization of terephthalate anions (TA^{2-}) intercalated CoMgAl LDHs.[72] Multiwalled, close-ended CNPs with a diameter of 10–35 nm and a length of 20–200 nm were formed from the intercalated TA^{2-} anions (Figure 3e). The in situ generated low-valence-state cobalt oxides acted as catalyst in the carbonization process, while the intercalated TA^{2-} anions were the solid-state carbon source for the formation of CNPs. Poly(vinyl sulfonate) intercalated CoAl LDHs were also reported to be effective for the fabrication of the LDO/CNPs nanocomposites.[73] The chemical composition and structure of the nanocomposites can be controlled by selecting chemical functional groups in the intercalated polymetric anions and varying processing conditions.

The structures and applications of the composites from LDHs and nanocarbon materials were extended by LDO/mesoporous carbon nanocomposites obtained through the carbonization of interlayer anions of LDHs. The carbonization is always carried out at high temperatures, which can destroy the hydrotalcite-like structure of LDHs, leaving metal oxides as the main products. However, LDHs are the kind of material in which the hydrotalcite-like structure can be reconstructed by rehydration after calcination.[42] It has been found that the reconstruction can be complete even if the LDH samples have been calcined at a temperature as high as 750 °C.[42] Hibino et al.[67] immersed the MgAl LDO/mesoporous carbon nanocomposites previously in a Na_2CO_3 aqueous solution for rehydration, and the well-ground calcined material was successfully regenerated to MgAl LDH/mesoporous carbon nanocomposites. Since most of the carbonization of interlayer anions of LDHs was conducted at a temperature of 400–600 °C, it provides the possibility for most of the as-obtained LDO/mesoporous carbon nanocomposites to be regenerated to their corresponding LDH/mesoporous carbon nanocomposites.

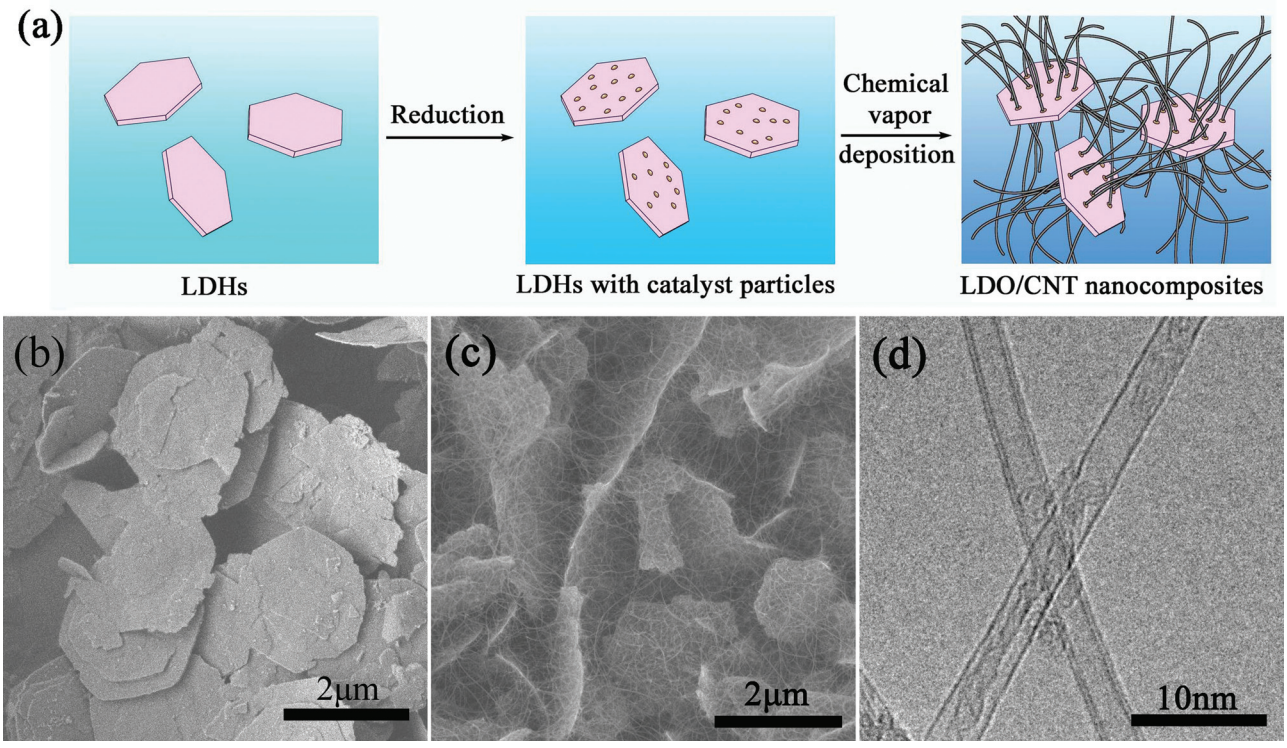

Figure 4. Growth of nanocarbon on LDHs: a) Schematic image of the formation of LDO/CNT nanocomposites from the in situ growth of S/DWCNTs with LDHs; b,c) SEM images of the LDH precursor (b) and the as-obtained LDO/CNT nanocomposites (c); d) TEM image of the as-grown S/DWCNTs in the LDO/CNT nanocomposites. Reproduced with permission.[13]

3.3.2. In Situ Growth of Nanocarbons with LDHs

Most transition metals, especially Fe, Co, and Ni, can be well arranged in lamellar LDH flakes on the atomic level. Calcination and reduction of LDHs give rise to their corresponding metal oxides or metal NPs with good dispersion, which can be used as excellent catalysts for the growth of nanocarbon materials. The physicochemical properties of such metal oxides or metal NPs (such as size, surface reactivity, and composition) can be well tuned through controllable calcination and reduction of LDHs and selection of the metal cation combination. Thus, various kinds of carbon materials, such as CNFs and CNTs, can be synthesized with LDHs as the catalyst precursor (**Figure 4**a). Furthermore, the lamellar structure of LDHs may also be preserved after the calcination and reduction processes, which facilitates the self-assembly of the as-grown nanocarbon materials with LDOs. As a result, hierarchical LDO/carbon material nanocomposites with various fascinating structures can be fabricated through the in situ growth of nanocarbons with LDHs.

As early as 1997, NiAl LDHs have been used as the catalyst for the growth of CNFs with a diameter of 15–69 nm from the decomposition of methane.[74] The irreducible domains such as Al_2O_3 were thought to be the primary reason for the high activity of the NiAl LDH catalyst due to their ability to enhance the dispersion of Ni NPs. When the CVD process was carried out in the absence of H_2, $NiAl_2O_4$ spinel particles will be formed from the NiAl LDHs, which were found to be catalytically active for the growth of novel submicrometer-scale flat CNFs.[75] CNFs can also grow in situ from LDHs with multiple transition metals, such as NiFeAl LDHs.[76] The content, nanostructure, and quality of the CNFs in the as-fabricated LDO/CNF nanocomposites were greatly influenced as a function of various parameters (such as hydrogen content, gas space velocity, and temperature).[77] In addition to the growth condition, the composition of LDHs also plays an important role in the structure of the as-fabricated LDO/carbon nanocomposites. The doping of a small amount of Cu into the NiAl LDH catalyst was found to be able to promote the activity, and more than 36 wt% of CNFs was produced when 2 mol% Cu was added into the NiAl LDHs with a Ni/Al molar ratio of 3:1. However, too much Cu was found to decrease the activity of the catalyst toward solid carbon formation.[78] Similar results were also reported when Cu was added into NiMgAl LDHs, which were also used as the catalyst for the growth of CNFs.[79] This can be attributed to the fact that the existence of Cu can enhance the hydrogen mobility and inhibit the formation of graphite layers on Ni surface.

With a better control of the reaction condition or the composition of the LDH precursor, CNTs, instead of CNFs, can be successfully synthesized from LDHs. For instance, by supporting NiAl LDHs on MWCNTs, Li et al.[80] successfully synthesized MWCNTs from NiAl LDHs with a diameter of 20–30 nm, which can be attributed to the fact that the interaction between the CNTs and NiAl LDOs kept the Ni particles from aggregating. Duan et al. successfully fabricated the CoAl LDO/MWCNT nanocomposites by the catalytic decomposition of acetylene over CoAl LDHs.[81] Further study indicated that the MWCNTs in the nanocomposites can evolve into caterpillar-like carbon fibers and carbon spheres with increasing growth

duration, leading to the formation of other kind of LDO/carbon nanocomposites.[82] LDHs with multiple transition metals, such as NiCr,[83] CoFeAl,[84] CoZnAl LDHs,[85] etc., were also used for the growth of MWCNTs to prepare LDO/MWCNT nanocomposites, indicating that the composition of LDOs in the as-obtained nanocomposites was controllable over a wide range. The change of the composition of LDHs also played an important role in the quality and yield of the as-grown CNTs. Hima et al.[86] found that the Co content in the CoAl LDH catalyst showed a significant influence on the structure of calcined LDHs and thus the growth of MWCNTs. The Co/Al molar ratio of 2.0 gave rise to much more uniform MWCNTs with higher graphitization due to a more uniform dispersion of active metallic Co NPs were obtained by reduction of the calcined products. Zhang et al. reported that, under the same growth condition, the incorporation of Mg into NiAl LDHs resulted in the growth of MWCNTs with a diameter of 15–25 nm, while CNFs with a diameter of 200–700 nm were obtained when NiAl LDHs were used as the catalyst.[75] With the increasing Mg/Al molar ratio in the LDH samples, the carbon content in the as-obtained LDO/MWCNT nanocomposites decreased and the specific surface areas of the composites increased remarkably. However, when the Mg/Ni molar ratio was too high, the specific surface area decreased strongly.[87]

Exploring efficient ways to robustly grow CNTs with fewer walls and smaller diameter, such as SWCNTs or double-walled CNTs (DWCNTs), requires very small metal NPs (less than 5 nm).[88] Fortunately, LDHs with low active phase (such as Fe, Co, Ni) were good precursors for S/DWCNT growth. Very recently, in situ growth of S/DWCNTs was achieved when Mg was incorporated into the LDH layers to stabilize the catalyst NPs and the growth condition was delicately controlled to prevent the small catalyst nanoparticles from sintering into larger ones due to the strong interaction between MgO and catalyst nanoparticles. Zhao et al.[89] reported the influence of different incorporated cations into FeMAl LDHs on the structure of the as-grown carbon nanomaterials, where M was divalent metal cation. It was found that with the same Fe content, SWCNTs were synthesized using a FeMgAl LDH catalyst, while MWCNTs and CNFs were obtained when FeZnAl and FeCuAl LDHs served as the catalysts, respectively. Note that most studies on the growth of nanocarbon materials with LDHs, focused on the yield and quality of the as-obtained nanocarbon materials. The structure of LDOs after the growth of nanocarbon materials was little concerned, and their content in the as-obtained products was too small to be noticed. Thus, nanocarbon materials, rather than LDO/carbon nanocomposites are much more representative for the products. Recently, we successfully fabricated the so-called LDO/CNT nanocomposites by growing S/DWCNTs using FeMgAl LDHs with different Fe contents as the catalyst precursor (Figure 4).[13] Both the wall number and diameter of the CNTs and the composition of the LDO flakes can be easily tuned by changing the proportion of Fe in the LDH flakes. It should be noted that the platelet-like structure of the LDH flakes were well preserved after the growth of CNTs. Thus, the as-obtained FeMgAl LDO/CNT nanocomposites exhibited a structure of S/DWCNTs interlinked with 2D flakes. CoMgAl, NiMgAl, as well as CoFeMgAl LDHs were also demonstrated to be excellent catalysts for the fabrication of LDO/SWCNT nanocomposites with similar structure. Compared with FeMgAl LDHs, CoMgAl, and NiMgAl LDHs showed a better selectivity to SWCNTs, but with lower content. The highest selectivity for metallic SWCNTs was obtained using CoMgAl LDHs as the catalyst. Furthermore, the growth of SWCNTs on Fe(Co, Ni)MgAl LDHs can also be carried out in a fluidized bed reactor, which significantly promoted the large scale production of the LDO/SWCNT nanocomposites.[90]

N-doped CNTs (NCNTs), which is a promising advanced functional material for catalysis and energy storage, can also be derived from the LDHs when nitrogen source was introduced during the CVD growth. NCNTs can be easily fabricated by pyrolysis of ethylenediamine with NiMgAl LDHs as the catalysts.[91] The N content and proportion of graphitic-like N structures increased with the increasing content of Ni in the LDH precursors. Large scale production of NCNTs with CoAl LDH catalyst by CVD at 850 °C under a mixture of methane and acetonitrile was reported.[92] CNTs with different N content were prepared by changing flow rates of methane and acetonitrile. Other kind of LDHs, such as MgFe[93–95] and CoMgAL LDHs,[95] were also used for the fabrication of LDO/NCNT nanocomposites.

If the pentagonal and heptagonal carbon rings can be periodically incorporated into the perfect hexagonal network of the graphitic sheet along the tube axis, coiled CNTs with helical structure can be grown. Zhang et al.[96] first reported that the addition of Mg can induce the formation of helical structured CNTs with an outer diameter of ca. 20 nm and that higher Mg content gives rise to the more helical CNTs. Later, the same group reported that single-helical CNFs with uniform coil diameter and coil pitches of about 80 nm were formed from NiCuAl LDHs, while double-helical CNFs with coil diameter of about 1–2 μm were observed over NiCuMgAl LDHs.[97] The double-helical CNFs were composed of two closely entwined fibers with equal helix pitch and an outer diameter of 200–300 nm, which were several micrometers to tens of micrometers in length. The formation of two types of helical CNFs were proposed to result from the diffusion of carbon species on different crystal planes of two different active metals (Ni and Cu), thus giving rise to two distinguishing deposition of graphitic layers.

When the catalyst NPs distributed on the LDO flakes were in high density, aligned CNTs, not randomly entangled CNTs, can be synchronously grown. For LDHs with large diameter and uniform size distribution, high-density Fe NPs (larger than 10^{15} m^{-2}) were embedded on both sides of FeMgAl LDO flakes by simple reduction of CO_3^{2-} intercalated FeMgAl LDH flakes. Aligned DWCNTs can synchronously grow and extend perpendicularly from both sides of the LDO flakes (**Figure 5**a and b).[98] Usually, thousands of LDH flakes were laid into the CVD reactor for aligned CNT growth. With continuous growth of the CNT arrays, the array tips met space resistance attributed from the neighboring flakes or CNT arrays. In order to minimize the stresses associated with the growth of CNTs, the arrays started to twist and coil on themselves around the ultralight LDO flakes (~0.2 ng), leading to the further assembly of CNT double helices with a length of tens of micrometers and a diameter of several micrometers. LDHs with a composition of FeCoMgAl–CO_3^{2-} were demonstrated to be effective for the growth of MWCNT double helices. To get CNTs with smaller diameter in double helix, we proposed a chemical precursor

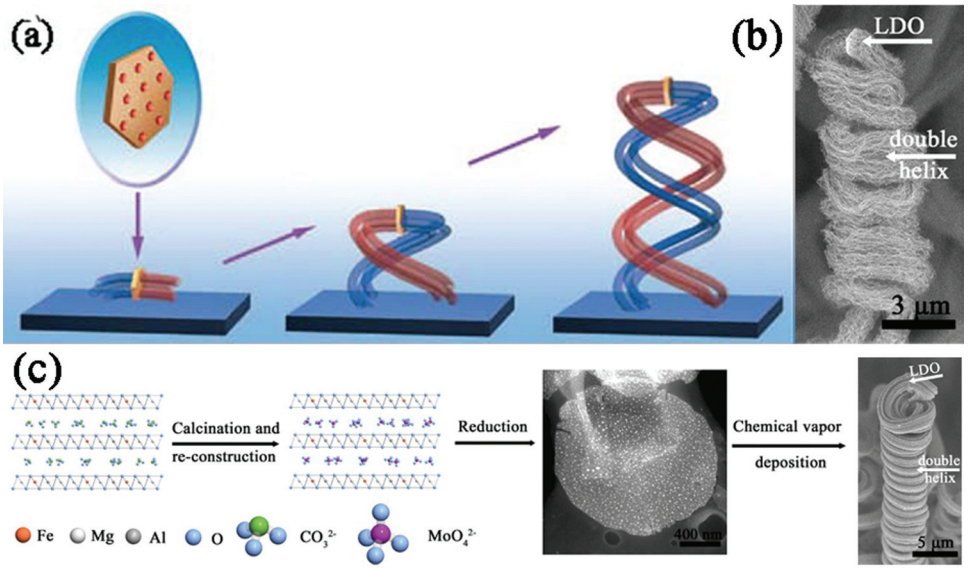

Figure 5. LDO/CNT double helices: a) Schematic image of the formation process of the double helical LDO/CNT array nanocomposites; b) SEM images of the double helical LDO/DWCNT array nanocomposites. Reproduced with permission.[98] c) Schematic image of the formation double helical LDO/SWCNT array nanocomposites by a chemical-precursor-mediated process, during which the intercalated CO_3^{2-} anions in FeMgAl LDHs were exchanged by MoO_4^{2-} anions. Reproduced with permission.[40] Copyright 2010, American Chemical Society.

mediated process based on the guest–host chemistry to form catalyst NPs with an extremely high density (10^{14} to 10^{16} m^{-2}), controllable size distribution (1–14 nm), and good thermal stability at high temperature (900 °C) from MoO_4^{2-} intercalated FeMgAl LDHs (Figure 5c).[40] A pinning effect of Mo around the Fe NPs was adopted to obtain a high density of small Fe NPs (over 10^{15} m^{-2}). The MoO_4^{2-} intercalated LDHs can also be easily prepared during the direct coprecipitation process.[99] These Fe NPs were active for the formation of SWCNT-array double helices on the as-obtained FeMoMgAl LDO flakes.

Table 3 summarized the synthesis methods and structure of the LDO/carbon nanocomposites mentioned above. Growth of nanocarbon materials from LDHs also demands for high temperatures that result in the damage of the hydrotalcite-like structure of the LDHs. Although in some cases, the platelet-like structure could be preserved, most parts of the as-obtained LDO flakes (such as metal NPs) was surrounded by graphene layers after the CVD growth. As a result, it is impossible for the LDO/carbon nanocomposites fabricated by this method to be regenerated into the corresponding LDH/carbon nanocomposites, which may hinder their applications in the field where the crystallinity of LDHs is necessary. However, this method shows the ability for the formation of various interesting structures based on LDOs and carbon materials. It should be highlighted that the formation of the double helical LDO/carbon nanostructures provides a new method of fabricating inorganic materials with double-helix structures by simple CVD.[100] This is an easy route to build 3D nanoarchitectures by bottom-up self-assembly strategy between 1D CNTs or CNFs and 2D flakes. Following studies on the chirality selectivity and alignment of such double helical/intercalated LDO/carbon nanocomposites are still to be carried out for further applications. Recently, other 2D clay, such as vermiculite,[8,101] montmorillonite,[5,102] as well as 3D sepiolite,[103] wallastonites,[104] and inorganic spheres,[105] can be used as substrate for nanocarbon deposition for 3D nanoarchitecture fabrication. Especially vertically aligned CNTs can be easily intercalated grown among vermiculite for alternate CNT/inorganic layer macrostructures by a facile CVD,[8,101] which is an efficient method for larger-scale integration of 1D and 2D materials. However, this kind of intercalated deposition does not take place if LDHs were employed as catalysts, because LDHs are hard to be exfoliated at high temperature. Pre-exfoliation of LDH flakes into single/double/multi-layered LDH nanosheets is a promising route to fully demonstrate the possibilities of 3D macrostructure assembly by in situ nanocarbon deposition, and the as-obtained nanocomposites show excellent material and physical properties, interesting for morphology-related applications, for instance, in micromechanics or nanoelectrodynamics.

In summary, many types of hierarchical LDH(LDO)/carbon nanocomposites derived from LDHs and various nanocarbons have been successfully fabricated to achieve a synergic combination of nanocarbons and LDHs. However, more efforts are still to be devoted towards the development of efficient structures, such as intercalation of CNTs into the interlayer space of LDHs, LDHs grown vertically to the graphene layer in situ, and graphene grown in situ on the surface of LDHs, etc., to maximally explore the combining properties of LDH(LDO)/carbon nanocomposites.

4. Application of LDH(LDO)/Carbon Nanocomposites

4.1. Energy Storage

Electricity, which is generated by various routes (such as thermal or hydraulic powered turbines, wind, and photovoltaic

Table 3. LDO/carbon nanocomposites obtained by the in situ growth of nanocarbon materials with LDHs.

Composition of LDHs	CVD Temperature [°C]	Carbon source	Type of deposited carbon	Carbon content [%]	Diameter [nm]	Ref.
NiAl	450–700	CH_4	CNFs	<98.8	15–69	[74]
NiAl	700	C_2H_2	CNFs	/	200–700	[75]
NiAl	650	C_3H_6	MWCNTs	/	20–30	[80]
CoAl	700	C_2H_2	MWCNTs	65.3–77.8	10–50	[81]
CoAl	700	C_2H_2	MWCNTs/CNFs/Carbon spheres	<99.2	30–40/100–130/150–180	[82]
NiCr	700	C_2H_2	MWCNTs	56.9	30–40	[83]
NiFeAl	600	C_2H_4/CO	CNFs	<98.8	19–45	[76]
NiFeAl	550–650	CO/C_2H_4	CNFs	<99.2	37–70	[77]
CoFeAl	700	C_2H_2	MWCNTs	55.6–77.8	10–18	[84]
CoZnAl	625	CH_4	MWCNTs	/	14–30	[85]
CoAl	700	C_2H_2	MWCNTs	65.3–77.8	10–50	[86]
NiCuAl	500–840	CH_4	CNFs	<98.7	10–60	[78]
NiCuMgAl	848–973	CH_4	CNFs	73.5	20–100	[79]
NiMgAl	700	C_2H_2	MWCNTs	77.8–87.0	15–25	
NiMgAl	650	C_3H_8	MWCNTs	73.8–93.7	36	[87]
FeMgAl	910	CH_4	SWCNTs	/	1.0–1.1	[89]
FeZnAl	910	CH_4	MWCNTs	/	15–50	[89]
FeCuAl	910	CH_4	CNFs	/	50–200	[89]
FeMgAl	900	CH_4	S/DWCNTs	15–36	1.0–6.0	[13]
CoMgAl	900	CH_4	SWCNTs	/	1.0–3.0	[90]
NiMgAl	900	CH_4	SWCNTs	/	1.0–6.0	[90]
NiMgAl	650	ethylenediamine	N-MWCNTs	/	15–80	[91]
CoAl	850	CH_4/acetonitrile	N-MWCNTs	84.8–86.2	20–60	[92]
MgFe	550-750	ethylenediamine	N-MWCNTs	/	20–50	[93]
MgFe	650	Hexane/ ethylenediamine	N-MWCNTs	/	20–70	[94]
CoMgAl/NiMgAl/MgFe	650	ethylenediamine	N-MWCNTs	/	20–50	[95]
NiMgAl	700	C_2H_2	MWCNTs	52.2–72.0	30–50	[96]
NiCuAl	700	C_2H_2	Helical CNFs	/	80	[97]
NiCuMgAl	700	C_2H_2	Double helical CNFs	/	200–300	[97]
FeMgAl	750	C_2H_4	Double helical DWCNTs	>95	5–7	[98]
(Fe)CoMgAl	750	C_2H_4	Double helical MWCNTs	/	/	[98]
FeMoMgAl	850/900	C_2H_4/C_3H_6	Double helical SWCNTs	>94	1–3	[40,99]

system), cannot be stored cheaply in large quantities, and more convenient and efficient ways for energy storage (such as electrochemical, electromagnetic, mechanical, thermal, and chemical route) are highly required. Among them, electrochemical energy storage, such as supercapacitors and Li–ion batteries, provides high energy or power density, good portability, and long cycling life for facile energy storage. Exploring advanced carbon-based energy materials is a good route to improve their performance and impetus their commercial applications.[106] Here, we take supercapacitor and Li-ion battery as examples to demonstrate the application of LDH(LDO)/carbon nanocomposites for energy storage.

4.1.1. Supercapactiors

Among various promising routes for energy storage, supercapacitors, also known as electrochemical supercapacitors or ultracapacitors, are gaining increasing attention for complementing batteries in hybrid electric vehicles, portable electronics, and industrial power management because of their large power density, moderate energy density, and longer cycle life. Due to the higher power capability and relatively larger energy density compared with conventional capacitors, supercapacitors offer a promising potential to meet the increasing power demands of energy storage systems. Exploring new

active electrode materials with good electrochemical performance has always been a major research topic for the development of supercapacitors. Carbon is the representative electrode material for the electric double-layered capacitor, the capacitance of which mainly arises from charges/ions stored in the electrode/electrolyte interface that is limited by the specific surface area of the electrode material and porosity accessible for ions transport.[107] Electrode materials with pseudo capacitive properties, such as metal hydroxides,[108] metal oxides,[109] and polymers,[110] are very promising for enhancing the performance of supercapacitors. Nanostructured carbon and their composites were good routes to take full use of the advantages of the double-layer capacitance and pseudo-capacitance. Further, some metal ions, such as Mn, Co, Ni, etc., can be well arranged into the LDH layers at an atomic level, which gives rise to their high activity for the faradic redox reaction. Therefore, LDH/carbon nanocomposites are considered as one of the most promising electrode materials for developing high-performance supercapacitors.

Various kinds of nanocarbons, such as CNTs, graphene, and activated carbon, were used with LDHs to fabricate hybrid supercapacitors with high performance. For instance, a CoAl LDH with an average particle size of 60–70 nm was used as a positive electrode for the asymmetric hybrid supercapacitor in combination with an active carbon negative electrode in KOH electrolyte solution. A specific capacitance of 77 F g^{-1} with a specific energy density of 15.5 Wh kg^{-1} was obtained for the hybrid supercapacitor within the voltage range of 0.9–1.5 V.[111] A concept of symmetric self-hybrid supercapacitors with composites consisting of CoAl LDHs mixed with MWCNTs as the electrode materials was proposed.[47] The two materials with distinct charge–storage mechanisms matched well as a composite. The work voltage for this new electrode material was prolonged in aqueous solution compared with either CoAl LDHs or MWCNTs, and the CV curves approached a rectangular shape. The LDH/MWCNTs nanocomposite electrodes exhibited better electrochemical performance and long-life cyclic stability at high current density than those with LDHs only. When 10 wt% MWCNTs were added, the specific capacitance increased from 192.0 F g^{-1} of pure CoAl LDHs to 342.4 F g^{-1} and the capacity retained 304 F g^{-1} after 400 cycles at a constant current of 2 A g^{-1}.[49] The better behavior of the composites can be attributed to the large surface area of MWCNTs and their good electronic conductivity, which consequently facilitated the access of ions in the electrolyte and electrons to the electrode/electrolyte interface.

When graphene was used as one of the building block for NiAl LDH/carbon nanocomposite,[61] a maximum specific capacitance of 781.5 F g^{-1} was observed, which is more than two folds than that of pure NiAl LDHs. The nanocomposites also exhibited an excellent cycle life with an increase of the specific capacitance of 22.6% compared with the initial capacitance. The enhancement was attributed to the combination of reversible electrochemical redox reaction from NiAl LDHs, the improved conductivity from graphene nanosheets, as well as the improved dispersion of graphene nanosheets from the incorporation of NiAl LDHs. To achieve a better combination of the properties for LDHs and nanocarbon materials, single-layer LDH/GO nanocomposites composed of face-to-face assembled single-layer CoAl LDHs and GO nanosheets were fabricated and used as the active electrode material for supercapacitors.[52] In the single-layer CoAl LDHs, all Co atoms were exposed on the surface, which maximized the activity for LDHs in a pseudocapacitive process. Furthermore, the face-to-face assembly of single-layer LDHs and GO nanosheets ensured a maximum contact of Co atoms and the graphene sheet, leading to a fast electron transport through graphene during the faradic redox reaction. Electrochemical studies performed on a three-electrode system showed that the single-layer LDH/GO nanocomposite electrode exhibited a high performance with specific capacitance of 1031 F g^{-1} at a current density of 1 A g^{-1} and could deliver an energy density of 7.7 Wh kg^{-1} at power density of 4.8 kW kg^{-1}. In addition, no obvious decrease of specific capacitance at a high current density of 20 A g^{-1} after more than 6000 cycles was observed in the galvanostatic charge and discharge curves (**Figure 6**).

Up to now, researches on the electrochemical properties of the LDH/carbon nanocomposites are still limited. In most cases, only CoAl LDHs were studied. It was found that only cobalt hydroxide component of CoAl LDHs could contribute to faradic redox reaction during electrochemical processes.[52] Recently, it has been reported that monometallic LDHs, such as $Co^{2+}Co^{3+}$ LDHs, can also be easily prepared and delaminated.[112] Such LDHs are speculated to be of much better pseudo capacitive properties than the CoAl LDHs. Besides, effective structures for the LDH/carbon nanocomposites that can maximize the combining electrochemical performance of the pseudo capacitive LDHs and double-layer capacitive nanocarbon materials, aiming at the development of next-generation supercapacitors which require light-weight, long cycle life, and high energy performance towards the level of ion batteries, are still to be explored.

4.1.2. Li-Ion Batteries

Li-ion batteries (LIBs), which consist of two electrodes that are capable of reversibly hosting Li in ionic form, have been widely accepted by industry for portable system. LIBs show advantages of high energy density, high operating voltage, long cycling life, good environment compatibility, and low self-discharge compared with traditional lead-acid and Ni-based batteries.[113] However, for the development of the newly emerging electronic devices, especially for electric vehicles or hybrid electric vehicles, there are still continuous demands for batteries with higher power and energy density and longer cycling life. The electrode material is one of the key issues for the high performance of LIBs. Carbon is the mostly used anode material for LIBs, and graphite-based anodes are the most commonly used commercial LIB anodes with a theoretical capacity of 372 mAh g^{-1}.[114] To improve the energy and power densities of LIBs, nanocarbons, such as 1D CNT/CNF, 2D graphene, and porous carbon, have been extensively explored as anode materials stimulated by their high specific surface area and excellent surface activities, which can create more active spaces or sites for Li storage.[115] Furthermore, various metals or metal oxides were integrated with nanocarbons to fabricate hierarchical nanocomposites to further improve their performance for LIBs.[113,115] This can be attributed to the factors that the as-fabricated nanocomposites

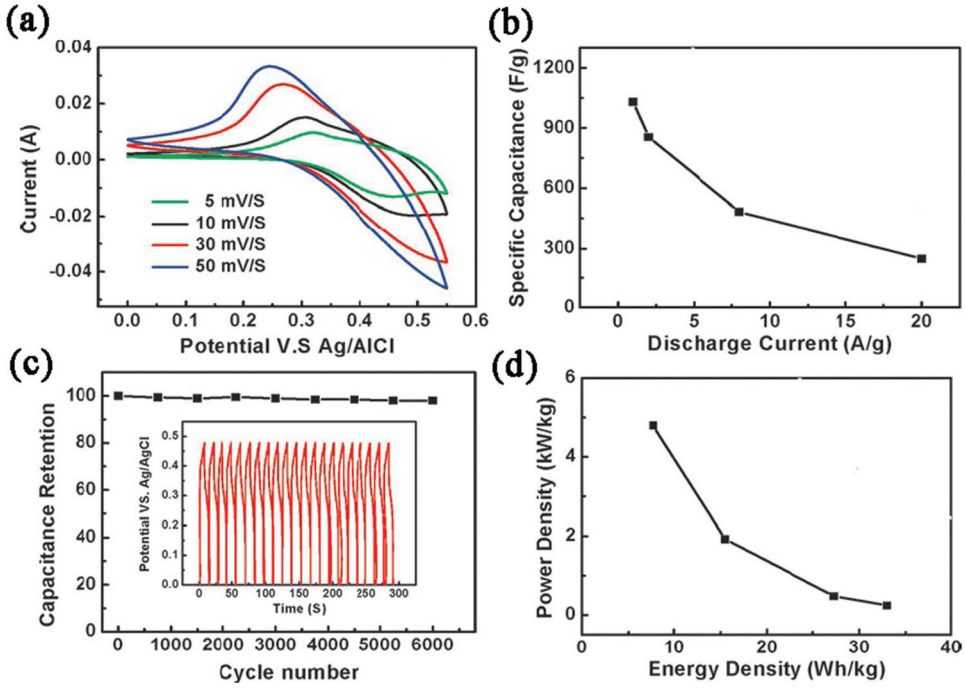

Figure 6. Application in energy conversion and storage: Electrochemical properties of LDH/GO nanocomposite: a) CV curves at various scan rates; b) specific capacitance of the composite at various discharge current densities; c) Galvanostatic charge and discharge curves and specific capacitance versus cycle number at a current density of 20 Ag^{-1}; d) Ragone plot based on the total mass of the composite. The energy and power densities were calculated from the galvanostatic discharge curves at various discharge current densities. Reproduced with permission.[52] Copyright 2011, Royal Society of Chemistry.

possess both the large Li-storage abilities of metal or metal oxide nanoparticles and nanocarbons, and the confinement of metal or metal oxide nanoparticles with nanocarbons can promote the dispersion of each other so as to improve the energy and power densities.[115] However, the effective connection of metal or metal nanoparticles with nanocarbons has always been a key issue for the fabrication of such nanocomposites.

In respect with the fact that most metal atoms (e.g., Mn, Co, Ni) can be well arranged into the LDH layers, and the calcination of these LDHs can lead to the formation of their corresponding metal oxides, which are high active anode materials for LIBs. Besides, the positively charged LDH flakes always exhibit strong interaction with the nanocarbons, which are usually with a negatively charged surface. Therefore, the LDH/nanocarbon composites are expected to be an excellent precursor to provide a strong interaction between metal oxides and nanocarbons, and thus can be used for the fabrication of high-performance metal oxide/nanocarbon composite LIB electrode materials. NiMn LDH/GO nanocomposites were obtained by co-precipitation method through mixing of colloidal suspensions of GO and exfoliated NiMn LDH nanosheets. Calcination of this kind of nanocomposites led to the reduction of GO into graphene by NiMn LDH, which was converted into the corresponding mixed oxides at the same time. It was noted that the as-obtained NiMn mixed oxide NPs were covered and wrapped by graphene layers, indicating the strong interaction between the graphene and metal oxides. This nanocomposite took advantages of the high conductivity from graphene as well as the good electrochemical response attributed from NiMn mixed oxides. Meanwhile, the aggregation of NiMn mixed oxides and the stacking of graphene layers were also effectively prevented the hierarchical structure of the NiMn mixed oxide/graphene nanocomposites. When this material was applied as the anode material for LIB, a maximum capacity of 1030 mAh g^{-1} was observed during the first discharge, and the capacity values were kept higher than 400 mAh g^{-1} after 10 cycles.[116] The fabrication of this material provides a way for the preparation of similar LDH/carbon nanocomposite-derived electrode materials with strong connection between metal oxides and nanocarbons, whose structure and composition can also be optimal for their performance in LIBs.

4.2. Material Science

Exploring high-performance polymer composites has always been a great challenge for material science. One of the most promising routes to prepare high-performance polymers is to add low-dimensional and nanoscale materials as nanofillers to improve their mechanical, electrical, and thermal properties. The 1D carbon nanomaterials, such as CNTs, are one of the mostly explored nanoscale fillers for fabrication of polymer nanocomposites due to their outstanding mechanical, electrical, and chemical properties.[2,117] As a subgroup of 2D nanostructured materials, LDHs with similar structure to clay minerals have also been widely used as nanofillers for the reinforcement of polymer composites.[37] However, the applications of both LDHs and CNTs are limited by their intrinsic properties, such

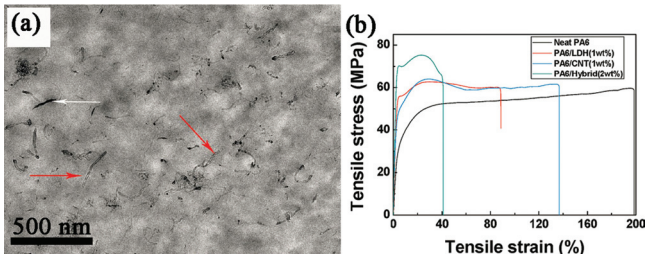

Figure 7. Application in materials science: a) TEM image of PA6/(LDH/CNT) nanocomposites; b) Typical stress-strain curves of neat PA6 and its nanocomposites. Reproduced with permission.[51] Copyright 2010, American Chemical Society.

as forming bundles or layered stacks when the surface is not modified due to the strong van der Waals interaction between the nanomaterials. The addition of 2D clay or LDH flakes into CNT suspension has been reported to be one of the most efficient methods that can significantly enhance both the dispersion of CNTs and flakes in the polymer matrix.[118] In addition, the combination of 1D nanotubes and 2D lamellar flakes leads to 3D hierarchical nanocomposites, which are with excellent performance far beyond those of the individual materials.[13] Therefore, the LDH(LDO)/CNT nanocomposites are promising in polymer reinforcement.

Du et al.[14] fabricated NiAl LDH/CNT nanocomposites through in situ growth of LDHs on CNTs, which were then used as a flame retardant for polypropylene (PP). The deposition of LDHs onto the surface of CNTs efficiently prevented CNTs from aggregating, and LDH itself also had a flame retardation effect. The LDH/CNT nanocomposites were proved to confer more excellent flame retardancy on PP composites with respect to LDHs and CNTs due to synergism of the barrier effect and the free radical trapping effect of the CNTs network. When single-layer LDH/CNT nanocomposites were employed as reinforcing nanofillers, both the LDHs and CNTs can be homogeneously dispersed in the polyamide 6 (PA6) matrix even at a high LDH/CNT content (2.0 wt%) due to the synergic effect of the LDH platelets and CNTs.[51] Compared to neat PA6, the tensile modulus of the PA6/(LDH/CNT) nanocomposites is increased by 210% from 1.0 to 3.1 GPa and the tensile strength is increased by 35% from 55.0 to 74.3 MPa, both of which are much higher than that of PA6/LDH or PA6/CNT system (**Figure 7**). Recently, we directly grew high-quality S/DWCNTs from LDHs while preserved their platelet-like morphology. The roots of the synthesized S/DWCNTs were fixed at certain spots of the LDO flakes, which thus prevented the aggregation of CNTs due to the orientating function. Furthermore, the interlinked S/DWCNTs also promoted the dispersion of LDO flakes. Therefore, the as-obtained LDO/CNT nanocomposites were demonstrated to be excellent fillers for strong polyimide (PI) films. It was found that the incorporation of only 0.40 wt% of such LDH/CNT nanocomposites significantly improved the mechanical properties of the PI film.[13] The elastic modulus of PI was improved by 18.4% from 651.3 to 770.9 MPa, and the tensile strength was improved by 39.7% from 78.1 to 109.1 MPa. The elongation-at-break of the composite film increased significantly by 124% from 26.6% to 59.6%, which is quite different from the decreasing trend for that of polymer/LDH or polymer/CNT nanocomposites.

Note that the size and composition of the LDH flakes can be easily controlled and the combination of LDHs and CNTs can be achieved in various hierarchical structures. The LDH(LDO)/CNT nanocomposites combining the synergic effect of LDH platelets and CNTs in material science can find promising applications for fabrication of high-performance and multifunctional polymer nanocomposites due to fine dispersion of the functional nanofillers and strong interactions with the matrix.

4.3. Catalysis

LDHs have been intensively investigated as the catalysts and catalyst supports for various kinds of chemical reactions due to the fact that a wide range of divalent, trivalent, even some univalent and tetravalent metal cations and almost all kinds of anions can be homogeneously arranged in their hydrotalcite-like layers or the interlayer spaces.[38,119] However, the catalytic activity of LDHs or the derived LDOs is always limited by their tendency to aggregate and poor mechanical properties. Various methods have been explored to overcome these problems, during which the combination with nanocarbon materials to form LDH(LDO)/carbon nanocomposites is one of the most concerned.

For the LDH/carbon nanocomposites that are obtained by reassembly of LDHs and carbon materials or in situ growth of LDHs on carbon, the intrinsic structure of LDHs is well retained. The carbon materials serve as the support for LDH catalysts to enhance their dispersion, heat, and mass transfer during the reaction, and offer the mechanical strength for the whole composites. Thus, the catalytic activity of LDHs in the LDH/carbon nanocomposites can be fully inherited or even improved. For instance, when NiAl LDH were in situ grown on MWCNTs, the as-obtained LDH/CNT nanocomposites were found to be an efficient catalyst for the further growth of large quantity of MWCNTs.[80] Winter et al.[59] investigated the activity of MgAl LDH/CNF nanocomposites from in situ growth of MgAl LDHs on the surface of CNFs for the catalytic synthesis of methyl isobutyl ketene from acetone. It was found that the specific activity of the as-obtained LDH/CNF nanocomposites in the self-condensation of acetone was more than four times higher than that of unsupported MgAl LDHs, leading to a great improvement in catalytic efficiency. Furthermore, when Pd NPs were deposited on the LDH/CNF nanocomposites, the initial activity of Pd-LDH/CNF in the condensation of acetone appeared to be five times higher than that measured with the physical mixture of MgAl LDHs and Pd-CNF. The activity in the dehydration reaction for the synthesis of methyl isobutyl ketone was also considerably higher, and the selectivity to desired products was improved from 95% for the physical mixture to more than 99%. Similar result was also reported for the electrocatalytic performance of NiAl LDH/CNT nanocomposites. Wang et al.[60] grew NiAl LDHs on MWCNTs in situ, and the electrode modified by the LDH/CNT nanocomposites exhibited eight times higher electrocatalytic activity for glucose electrooxidation than those modified by either pristine LDHs or CNTs (**Figure 8**). The enhanced electrocatalytic activity of the LDH/CNT nanocomposites was attributed to the facts that CNTs can efficiently

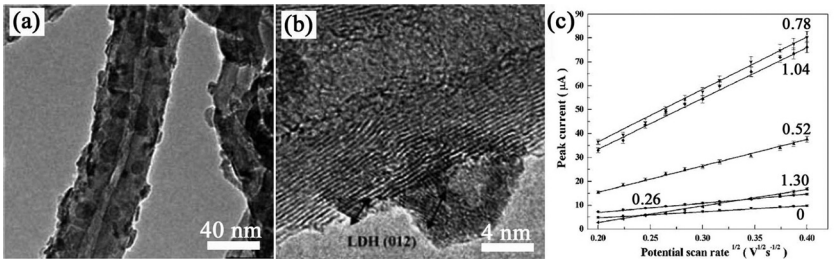

Figure 8. Application in catalysis: a,b) TEM (a) and high-resolution TEM (b) images of NiAl LDH/CNT nanocomposites; c) Peak current as a function of the square root of scan rate showing the electroactivity of NiAl LDH/CNT composites with different mass ratio of CNTs to LDHs for glucose electrooxidation. Reproduced with permission.[60] Copyright 2010, Royal Society of Chemistry.

promote the charge transport between the active Ni centers and the electrode and the CNTs also constructed a porous network-like structure to enhance the diffusion of the reactant.

For LDO/carbon nanocomposites obtained by the carbonization of interlayer anions of LDHs and direct growth of carbon materials from LDHs, the catalytic active metal particles or metal oxides are always surrounded with carbon layers which seriously inhibited their activity. However, the carbon materials derived from the LDHs with interesting structures can be used as excellent catalyst supports. For instance, Zhang et al.[75] synthesized CNFs with submicrometer-scale flat structure or with coiled structure, and they were used as effective catalyst supports for electrooxidation of methanol. After the loading of Pt, such electrocatalyst exhibited much higher activity and better anti-poisoning ability than the commercial Pt/carbon black catalyst, which was believed to be the combined beneficial effects of the novel microstructure and composition of the as-obtained LDO/CNF nanocomposites. CNFs with special microstructure greatly facilitated the deposition and dispersion of Pt NPs and promoted the diffusion of the reactant. The LDOs in the composites can absorb oxygen-containing species, which reacted with carbonyl-containing species of methanol products on the Pt surface to produce CO_2 and release the active sites of Pt for further methanol oxidation.

The exploration of hierarchical architecture of LDH/nanocarbon in heterogeneous and electrochemical catalysis is under progress. Compared with traditional catalyst prepared by co-precipitation or loading method, the metal phase in the LDHs is an atomic dispersion. The as-obtained hierarchical nanocomposites exhibit mediated macro-, meso-, and micropores, and the required active sites are expected to be distributed on the internal surface to effectively catalyze the reaction. With the novel understanding on carbon and metal oxide catalysis, potential catalysts based on LDH/nanocarbon for dehydrogenation, oxidation, and C–H activation will be developed.

4.4. Environment Protection

The pollution of water resources due to the indiscriminate disposal of numerous inorganic (e.g., heavy metal cations or anions) and organic (e.g., dyes, oils) contaminants from industries and human life has been causing worldwide concern. It is necessary to remove these contaminants from the waters before release into the environment. There are various methods that are being employed to remove these contaminants including oxidation, reduction, precipitation, membrane filtration, ion/anion exchange, and adsorption, among which adsorption is the most promising process for the removal of contaminants from wastewater due to its effectiveness and low cost. Nanocarbons, especially for CNTs, are considered to be one of the most promising candidates for oil and metal cations adsorption. There is a high degree of π-electron delocalization in the conjugated system on the surface of CNTs due to the sp^2 hybridization of carbon atoms, which gives rise to the strong interaction between CNTs and aromatic compounds by π–π electron coupling/stacking effect. Besides, the existence of large quantities of pore structures makes CNTs a great absorber with high adsorption capacity for neutral organic or oil pollutants.[7,120,121] Furthermore, it has been reported that CNTs with designed structures, such as aligned CNTs or CNT sponge, can be repeatedly compressed and recovered in thousands of cycles.[8,120,122] The compression of CNTs can lead to the release of the adsorbed pollutants, indicating the excellent recycling performance of CNTs for oil adsorption. The functionalized CNTs exhibit high adsorption capacity for various kinds of metal cations attributed from their negatively charged surface.[123]

Owing to their large surface area, positively charged layers, and extraordinary anion-exchange properties, LDHs have been widely explored as adsorbent materials for the removal of anionic contaminants for aqueous solutions. LDHs exhibit high adsorption capacities for both inorganic (e.g., F^-, SO_4^{2-}, AsO_4^{3-}, $Cr_2O_7^{2-}$) and organic (e.g., aromatic carboxylic acids, phenols, pesticides) anions.[119] LDHs can take up anion contaminants from solution mainly by three different mechanisms: surface adsorption, interlayer anion exchange, and reconstruction of their hydrotalcite-like structure of calcined LDHs. Anions can be easily adsorbed on the positively charged surface of LDHs. The anion exchange capacity of LDHs is affected by the nature of initial interlayer anions and the layer charge density. LDHs exhibit greater affinities for multivalent anions compared with monovalent anions. The anion-exchange capacity decreases with the higher layer charge density of LDHs due to the stronger interaction between the initial interlayer anions and the positively charged layers.[124] Calcination can lead to the decomposition of interlayer anions of LDHs, and the as-obtained LDOs are usually with much higher adsorption capacity for anionic contaminants during the reconstruction.[125] Therefore, calcination and reconstruction processes provide a great potential to reuse and recycle the adsorbent. Great efforts have been devoted to improve the adsorption properties for cations and neutral organic molecules. Surface modifications to add negatively charged functional groups or chelating agents were carried out to provide the adsorption capacity of metal cations for LDHs.[126] By intercalating large organic anions, such as surfactants, into the interlayer of LDHs, the LDH surface properties of LDHs were changed from hydrophilic to hydrophobic, resulting in the enhanced adsorption capacity of LDHs for a diverse range of organic pollutants and even non-ionic organic

materials.[127] However, the adsorption capacities of the modified LDHs for cations and neutral organic molecules are still limited, and the modification processes are complicated.

Contaminants that need to be treated are always complex. For instance, waste waters from human life and many industries such as metallurgical, chemical manufacturing, mining, battery manufacturing, etc., contain not only the cationic heavy metals, but also various kinds of anionic molecules, neutral organic, or oil pollutants. All of these contaminants have to be removed before the sewage can be discharged. In sewage treatment process, there always several steps to remove these contaminants one by one, sequentially. Here, the LDH/carbon nanocomposites, especially for those fabricated by in situ growth of LDHs on CNTs, can not only inherit the anion-exchange properties of LDHs, but also preserve the hydrophobic and porosity of nanocarbons. Therefore, the LDH/carbon nanocomposites are promising materials with excellent performance for the removal of all the cationic, anionic, neutral, inorganic, and organic contaminants in a single-batch system by adsorption. However, few reports on the adsorption of LDH/carbon nanocomposites have been reported, and relative studies are still to be carried out.

4.5. Drug Delivery

Since their discovery, nanocarbons such as CNTs and graphene have been considered to be advanced nanovectors for the highly efficient delivery of drugs owing to their large surface and unique optical and electrical properties.[128,129] Pristine nanocarbons cannot be employed directly for drug delivery, and functionalization must be adopted to improve their biocompatibility and solubility, which also allows further modification of the nanocarbon material with drugs. Drugs containing aromatic groups can be easily bonded to nanocarbon non-covalently by strong π–π interactions. The negatively charged surface of functionalized nanocarbons could improve their conjugation with positively charged drug molecules and the binding to a single cell by interacting through multiple binding sites due to their flexibility. The nanocarbon cellular uptake mechanism may differ depending on the functionalization and size of the nanocarbons, including endocytosis,[130] and passive diffusion.[131] The intrinsic optical and electrical properties of nanocarbon can be specially utilized in imaging and therapeutic applications to reveal the details of cellular delivery process.[129] Due to a large specific surface area, nanocarbon allows multi-conjugation of various molecules on the sidewalls, including drugs, targeting moieties, and fluorescein.[132] Thus, the targeting-specific delivery of drugs can be conducted under in situ detection. However, the drug-delivery efficiency of nanocarbons is still limited by their toxicity and tendency to aggregation and the difficulty to control the drug release process.

Taking advantages of their biocompatibility, anion-exchange ability, and low cytotoxicity, LDHs are also endowed with great potential as inorganic NPs for drug delivery.[119,133] Various anionic pharmaceutically active compounds can be intercalated into the interlayer space of LDHs by anion-exchange. The interlayer region of LDHs can be considered as a microvessel, where the drug is stored while maintaining its integrity and is protected from the reaction of light and oxygen. After the cellular uptake of LDH-drug particles by clathrin-mediated endocytosis, the drug may be released through a deintercalation process because of anion exchange or displacement reactions. The release of drug is controllable by the strength of the host–guest interaction, the rigidity of LDH layers and the diffusion path length, which is of paramount importance to maintain pharmacologically active drug levels for long periods and avoiding repeated drug administration. After surface modification with targeting moieties, targeting-specific drug delivery by LDHs can also be achieved.[134] However, the tendency to aggregation of LDH particles may limit the cellular uptake process, and may also lead to the loss of the target delivery. Besides, it is still a challenge to fully understand the cellular delivery process, including the approach and adhesion to cell membrane, LDH particle endocytosis, and the release of drugs, etc.

Considering the synergic effect, LDH/carbon nanocomposites are also expected to be a promising drug-delivery vector with high performance. The kinds of drug that are delivered can be extended, and the cytotoxicity of nanocarbons may be lowered by the modification of LDHs. The nanocomposites are also expected to combine the controllable drug release of LDHs and the advantage of nanocarbon to allow for imaging. Since the combination of nanocarbon and LDHs is able to enhance the dispersion of each other, the drug-delivery efficiency of the LDH/carbon nanocomposites is also expected to be improved.

5. Conclusions

Various kinds of hierarchical LDH(LDO)/carbon nanocomposites have been successfully fabricated from the combination of LDHs and different kinds of nanocarbons. The LDH/carbon nanocomposites obtained by reassembly of LDHs and carbon materials or by the in situ growth of LDH flakes on carbon materials can fully inherit the properties of both LDHs and carbon materials. They may even exhibit improved or unexpected properties due to their unique structures. The carbonization of interlayer anions of LDHs or CVD growth of nanocarbon materials from LDHs always lead to the formation of LDO/carbon nanocomposites, in which the hydrotalcite-like structure of LDHs has been destroyed, leaving metal oxides or some spinel phase as the main component. However, very interesting structures, such as micro/mesoporous structure and single/double helical structure, can be derived through these two methods. Note that the LDO/carbon nanocomposites from the carbonization of interlayer anions of LDHs exhibit the possibility to be regenerated into their corresponding LDH/carbon nanocomposites due to the intermediate temperature demanded for the carbonization.

The carbon materials in the LDH(LDO)/carbon nanocomposites can serve as the support for the dispersion of LDH flakes and provide the conductivity for the composites, while the existence of LDHs or LDOs provide the chemical activity and can also enhance the dispersion of nanocarbon materials. Therefore, compared to either LDHs or nanocarbon materials, the combined LDH(LDO)/carbon nanocomposites are with much better performance when they were used as electrode materials, nanofillers for polymer reinforcement, and catalysts

or catalyst supports. The LDH(LDO)/carbon nanocomposites are also promising towards applications in adsorption and drug delivery with high performance.

6. Outlook

Reassembly of nanocarbons and LDHs, formation of LDHs on nanocarbons, and formation of nanocarbons on LDHs by carbonization of the interlayer anions of LDHs or in situ CVD growth of nanocarbons with LDHs were efficient and effective routes for LDH(LDO)/carbon nanocomposite fabrication. However, none of them can precisely manipulate the LDH/LDO flakes or nanocarbons into arbitrary nanoarchitectures. The multiobject interactions between the complex building blocks are still too complex, and nonlinear behavior maybe presented. The materials and physical chemistry during nanocomposite fabrication, such as the interactions between nanocarbons and LDH/LDO flakes, the electron transfer, and its response to light, electric, or magnetic field, is still an open question. Recently, integrating 1D nanotube growth on 2D LDH flaks lead to the formation of a 3D double helix, similar to that of natural DNA and proteins, providing a novel structural platform as the prototype for nanoeletronmagnetic Faraday coils for nano-electromechanical systems. It also opens great opportunities for novel hierarchical nanoarchitectures fabrication via bottom-up self-organization. However, new insights on these materials chemistry and physics are quite important to provide a general understanding for controllable atomic-by-atomic self-assembly or chemical reaction for nanoarchitecture building and the relationship between the structure and their properties.

Up to now, many kinds of metals (e.g., Li, Mg, Al, Ca, Ti, Mn, Fe, Co, Ni, Zn, Ga, In) can be dispersed on the atomic level in a lamellar LDH flake with controllable components. However, for most of the investigated LDH/carbon nanocomposites, only MgAl, CoAl, and NiAl LDHs were used. Further investigations on using LDHs with unique composition and properties to fabricate LDH/carbon nanocomposites for the development of multifunctional materials with excellent properties and promising applications are still to be carried out. The current studies on the LDO/carbon nanocomposites fabricated by the direct formation of nanocarbons on LDHs mostly focused on the yield and quality of the as-obtained carbon materials, rather than the structure to maximize the properties of the composites. Besides, note that the LDH flakes can be easily delaminated into single-layer LDHs. With the recent rise attention of graphene, as another kind of one-atomic-thick material, the as-obtained single-layer LDHs have undoubtedly become one of the hottest topics for material science. More researches on the fabrication and application of single-layer LDH/carbon nanocomposites to maximize the properties of different kinds of single-layer LDHs and carbon materials are still to be carried out in the near future.

Furthermore, the combination of CNTs, graphene, and LDH(LDO) is expected to be able to provide more opportunities for advanced hierarchical macrostructures, however, the interaction among them will be more complex, and precise structure modulation is still a great challenge. The hierarchical designs, as well as other LDH/nanocarbon hybrids illustrated in Scheme 2, are promising advanced functional materials that can be used in areas such as nanoelectronic, magnetic devices, catalysis, separation, materials science, energy conversion and storage, catalysis, environmental, biology, and human health. To realize this goal, new insights on relationship between the structure, property, and applications are always required. If some bulk application can be visualized, more efforts should be devoted on their delicate structural modulation and mass production at a low cost, such as hierarchical nanocomposite electrode for supercapacitor and Li-ion battery.

Acknowledgements

The work was supported by the National Basic Research Program of China (No. 2011CB932602) and the Foundation for the Natural Scientific Foundation of China (No. 20736007, No. 2007AA03Z346).

Received: September 19, 2011
Published online: January 9, 2012

[1] a) E. P. Giannelis, *Adv. Mater.* **1996**, *8*, 29; b) A. Okada, A. Usuki, *Macromol. Mater. Eng.* **2006**, *291*, 1449; c) Q. H. Zeng, A. B. Yu, G. Q. Lu, D. R. Paul, *J. Nanosci. Nanotechnol.* **2005**, *5*, 1574.
[2] a) M. Moniruzzaman, K. I. Winey, *Macromolecules.* **2006**, *39*, 5194; b) J. N. Coleman, U. Khan, Y. K. Gun'ko, *Adv. Mater.* **2006**, *18*, 689.
[3] a) V. P. Veedu, A. Y. Cao, X. S. Li, K. G. Ma, C. Soldano, S. Kar, P. M. Ajayan, M. N. Ghasemi-Nejhad, *Nat. Mater.* **2006**, *5*, 457; b) T. Byrne, Y. K. Gun'ko, *Adv. Mater.* **2010**, *22*, 1672; c)L. Q. Liu, W. J. Ma, Z. Zhang, *Small* **2011**, *7*, 1504.
[4] H. Bai, C. Li, G. Q. Shi, *Adv. Mater.* **2011**, *23*, 1089.
[5] W. D. Zhang, I. Y. Phang, T. X. Liu, *Adv. Mater.* **2006**, *18*, 73.
[6] F. C. C. Moura, R. M. Lago, *Appl. Catal. B* **2009**, *90*, 436.
[7] M. Q. Zhao, J. Q. Huang, Q. Zhang, W. L. Luo, F. Wei, *Appl. Clay Sci.* **2011**, *53*, 1.
[8] Q. Zhang, M. Q. Zhao, Y. Liu, A. Y. Cao, W. Z. Qian, Y. F. Lu, F. Wei, *Adv. Mater.* **2009**, *21*, 2876.
[9] S. H. Lee, D. H. Lee, W. J. Lee, S. O. Kim, *Adv. Funct. Mater.* **2011**, *21*, 1338.
[10] a) Z. J. Fan, J. Yan, L. J. Zhi, Q. Zhang, T. Wei, J. Feng, M. L. Zhang, W. Z. Qian, F. Wei, *Adv. Mater.* **2010**, *22*, 3723; b) S. S. Li, Y. H. Luo, W. Lv, W. J. Yu, S. D. Wu, P. X. Hou, Q. H. Yang, Q. B. Meng, C. Liu, H. M. Cheng, *Adv. Energy Mater.* **2011**, *1*, 486; c) X. H. Cao, Q. Y. He, W. H. Shi, B. Li, Z. Y. Zeng, Y. M. Shi, Q. Y. Yan, H. Zhang, *Small* **2011**, *7*, 1199; d) L. L. Zhang, Z. G. Xiong, X. S. Zhao, *ACS Nano* **2010**, *4*, 7030.
[11] D. G. Evans, R. C. T. Slade, *Struct. Bond.* **2006**, *119*, 1.
[12] H. J. Li, G. Zhu, Z. H. Liu, Z. P. Yang, Z. L. Wang, *Carbon* **2010**, *48*, 4391.
[13] M. Q. Zhao, Q. Zhang, X. L. Jia, J. Q. Huang, Y. H. Zhang, F. Wei, *Adv. Funct. Mater.* **2010**, *20*, 677.
[14] B. X. Du, Z. P. Fang, *Nanotechnology* **2010**, *21*, 315603.
[15] A. Krishnan, E. Dujardin, T. W. Ebbesen, P. N. Yianilos, M. M. J. Treacy, *Phys. Rev. B* **1998**, *58*, 14013.
[16] M. F. Yu, O. Lourie, M. J. Dyer, K. Moloni, T. F. Kelly, R. S. Ruoff, *Science* **2000**, *287*, 637.
[17] M. F. Yu, B. S. Files, S. Arepalli, R. S. Ruoff, *Phys. Rev. Lett.* **2000**, *84*, 5552.
[18] J. W. G. Wildoer, L. C. Venema, A. G. Rinzler, R. E. Smalley, C. Dekker, *Nature* **1998**, *391*, 59.
[19] T. W. Ebbesen, H. J. Lezec, H. Hiura, J. W. Bennett, H. F. Ghaemi, T. Thio, *Nature* **1996**, *382*, 54.

[20] a) S. Berber, Y. K. Kwon, D. Tomanek, *Phys. Rev. Lett.* **2000**, *84*, 4613; b) P. Kim, L. Shi, A. Majumdar, P. L. McEuen, *Phys. Rev. Lett.* **2001**, *87*, 215502.
[21] M. Endo, M. S. Strano, P. M. Ajayan, *Top. Appl. Phys.* **2008**, *111*, 13.
[22] A. Peigney, C. Laurent, E. Flahaut, R. R. Bacsa, A. Rousset, *Carbon* **2001**, *39*, 507.
[23] a) K. Metenier, S. Bonnamy, F. Beguin, C. Journet, P. Bernier, M. L. de La Chapelle, O. Chauvet, S. Lefrant, *Carbon* **2002**, *40*, 1765; b) K. M. Liew, C. H. Wong, X. Q. He, M. J. Tan, *Phys. Rev. B* **2005**, *71*, 075424.
[24] A. K. Geim, K. S. Novoselov, *Nat. Mater.* **2007**, *6*, 183.
[25] C. Lee, X. D. Wei, J. W. Kysar, J. Hone, *Science* **2008**, *321*, 385.
[26] J. H. Chen, C. Jang, S. D. Xiao, M. Ishigami, M. S. Fuhrer, *Nat. Nanotechnol.* **2008**, *3*, 206.
[27] J. H. Seol, I. Jo, A. L. Moore, L. Lindsay, Z. H. Aitken, M. T. Pettes, X. S. Li, Z. Yao, R. Huang, D. Broido, N. Mingo, R. S. Ruoff, L. Shi, *Science* **2010**, *328*, 213.
[28] Y. W. Zhu, S. Murali, W. W. Cai, X. S. Li, J. W. Suk, J. R. Potts, R. S. Ruoff, *Adv. Mater.* **2010**, *22*, 3906.
[29] a) S. Banerjee, T. Hemraj-Benny, S. S. Wong, *Adv. Mater.* **2005**, *17*, 17; b) K. P. Loh, Q. L. Bao, P. K. Ang, J. X. Yang, *J. Mater. Chem.* **2010**, *20*, 2277.
[30] S. J. Guo, S. J. Dong, *Chem. Soc. Rev.* **2011**, *40*, 2644.
[31] a) M. Terrones, A. G. Souza, A. M. Rao, *Top. Appl. Phys.* **2008**, *111*, 531; b) P. Ayala, R. Arenal, M. Rummeli, A. Rubio, T. Pichler, *Carbon* **2010**, *48*, 575; c) D. S. Su, J. Zhang, B. Frank, A. Thomas, X. C. Wang, J. Paraknowitsch, R. Schlogl, *ChemSusChem* **2010**, *3*, 169.
[32] X. D. Shi, A. R. Kortan, J. M. Williams, A. M. Kini, B. M. Savall, P. M. Chaikin, *Phys. Rev. Lett.* **1992**, *68*, 827.
[33] T. L. Makarova, *Semiconductors* **2001**, *35*, 243.
[34] R. C. Haddon, A. S. Perel, R. C. Morris, T. T. M. Palstra, A. F. Hebard, R. M. Fleming, *Appl. Phys. Lett.* **1995**, *67*, 121.
[35] R. C. Yu, N. Tea, M. B. Salamon, D. Lorents, R. Malhotra, *Phys. Rev. Lett.* **1992**, *68*, 2050.
[36] a) S. Velu, N. Shah, T. M. Jyothi, S. Sivasanker, *Micropor. Mesopor. Mat* **1999**, *33*, 61; b) W. T. Reichle, S. Y. Kang, D. S. Everhardt, *J. Catal.* **1986**, *101*, 352; c) F. M. Labajos, V. Rives, M. A. Ulibarri, *J. Mater. Sci.* **1992**, *27*, 1546.
[37] a) D. G. Evans, D. A. Xue, *Chem. Commun.* **2006**, 485; b) L. C. Du, B. J. Qu, *J. Mater. Chem.* **2006**, *16*, 1549; c) A. Illaik, C. Taviot-Gueho, J. Lavis, S. Cornmereuc, V. Verney, F. Leroux, *Chem. Mater.* **2008**, *20*, 4854.
[38] Z. P. Xu, J. Zhang, M. O. Adebajo, H. Zhang, C. H. Zhou, *Appl. Clay Sci.* **2011**, *53*, 139.
[39] a) F. Z. Zhang, X. Xiang, F. Li, X. Duan, *Catal. Surv. Asia* **2008**, *12*, 253; b) D. P. Debecker, E. M. Gaigneaux, G. Busca, *Chem. Eur. J.* **2009**, *15*, 3920.
[40] M. Q. Zhao, Q. Zhang, W. Zhang, J. Q. Huang, Y. H. Zhang, D. S. Su, F. Wei, *J. Am. Chem. Soc.* **2010**, *132*, 14739.
[41] a) Y. Wang, W. S. Yang, S. C. Zhang, D. G. Evans, X. Duan, *J. Electrochem. Soc.* **2005**, *152*, A2130; b) X. M. Liu, Y. H. Zhang, X. G. Zhang, S. Y. Fu, *Electrochim. Acta* **2004**, *49*, 3137; c) Y. G. Wang, L. Cheng, Y. Y. Xia, *J. Power Sources* **2006**, *153*, 191.
[42] J. Rocha, M. del Arco, V. Rives, M. A. Ulibarri, *J. Mater. Chem.* **1999**, *9*, 2499.
[43] a) F. Leroux, C. Taviot-Gueho, *J. Mater. Chem.* **2005**, *15*, 3628; b) Y. F. Wang, H. Z. Gao, *J. Colloid Interf. Sci* **2006**, *301*, 19; c) M. Z. bin Hussein, Z. Zainal, A. H. Yahaya, D. W. V. Foo, *J. Control Release.* **2002**, *82*, 417; d) L. Tammaro, U. Costantino, M. Nocchetti, V. Vittoria, *Appl. Clay. Sci.* **2009**, *43*, 350.
[44] a) E. Delahaye, S. Eyele-Mezui, J. F. Bardeau, C. Leuvrey, L. Mager, P. Rabu, G. Rogez, *J. Mater. Chem.* **2009**, *19*, 6106; b) J. B. Han, D. P. Yan, W. Y. Shi, J. Ma, H. Yan, M. Wei, D. C. Evans, X. Duan, *J. Phys. Chem. B* **2010**, *114*, 5678.
[45] a) S. O'Leary, D. O'Hare, G. Seeley, *Chem. Commun.* **2002**, 1506; b) T. Hibino, W. Jones, *J. Mater. Chem.* **2001**, *11*, 1321.
[46] H. L. Wang, H. S. Casalongue, Y. Y. Liang, H. J. Dai, *J. Am. Chem. Soc.* **2010**, *132*, 7472.
[47] L. H. Su, X. G. Zhang, C. Z. Yuan, B. Gao, *J. Electrochem. Soc.* **2008**, *155*, A110.
[48] W. Y. Tseng, J. T. Lin, C. Y. Mou, S. F. Cheng, S. B. Liu, P. P. Chu, H. W. Liu, *J. Am. Chem. Soc.* **1996**, *118*, 4411.
[49] L. H. Su, X. G. Zhang, Y. Liu, *J. Solid State Electrochem.* **2008**, *12*, 1129.
[50] a) L. Li, R. Z. Ma, Y. Ebina, N. Iyi, T. Sasaki, *Chem. Mater.* **2005**, *17*, 4386; b) Z. P. Liu, R. Z. Ma, M. Osada, N. Iyi, Y. Ebina, K. Takada, T. Sasaki, *J. Am. Chem. Soc.* **2006**, *128*, 4872; c) R. Z. Ma, Z. P. Liu, L. Li, N. Iyi, T. Sasaki, *J. Mater. Chem.* **2006**, *16*, 3809.
[51] S. Huang, H. D. Peng, W. W. Tjiu, Z. Yang, H. Zhu, T. Tang, T. X. Liu, *J. Phys. Chem. B* **2010**, *114*, 16766.
[52] L. Wang, D. Wang, X. Y. Dong, Z. J. Zhang, X. F. Pei, X. J. Chen, B. A. Chen, J. Jin, *Chem. Commun.* **2011**, *47*, 3556.
[53] a) S. Srivastava, N. A. Kotov, *Accounts. Chem. Res.* **2008**, *41*, 1831; b) Y. Wang, A. S. Angelatos, F. Caruso, *Chem. Mater.* **2008**, *20*, 848; c) E. Kharlampieva, S. A. Sukhishvili, *Polymer Rev.* **2006**, *46*, 377.
[54] a) J. H. Lee, S. W. Rhee, D. Y. Jung, *J. Am. Chem. Soc.* **2007**, *129*, 3522; b) J. B. Han, X. Y. Xu, X. Y. Rao, M. Wei, D. G. Evans, X. Duan, *J. Mater. Chem.* **2011**, *21*, 2126; c) D. P. Yan, J. Lu, M. Wei, J. B. Han, J. Ma, F. Li, D. G. Evans, X. Duan, *Angew. Chem. Int. Ed.* **2009**, *48*, 3073.
[55] a) M. N. Zhang, Y. M. Yan, K. P. Gong, L. Q. Mao, Z. X. Guo, Y. Chen, *Langmuir.* **2004**, *20*, 8781; b) S. W. Lee, B. S. Kim, S. Chen, Y. Shao-Horn, P. T. Hammond, *J. Am. Chem. Soc.* **2009**, *131*, 671; c) D. W. Lee, T. K. Hong, D. Kang, J. Lee, M. Heo, J. Y. Kim, B. S. Kim, H. S. Shin, *J. Mater. Chem.* **2011**, *21*, 3438; d) B. S. Kong, J. X. Geng, H. T. Jung, *Chem. Commun.* **2009**, 2174; e) X. Zhao, Q. H. Zhang, Y. P. Hao, Y. Z. Li, Y. Fang, D. J. Chen, *Macromolecules.* **2010**, *43*, 9411.
[56] D. Chen, X. Y. Wang, T. X. Liu, X. D. Wang, J. Li, *ACS Appl. Mater. Interfaces* **2010**, *2*, 2005.
[57] J. He, M. Wei, B. Li, Y. Kang, D. G. Evans, X. Duan, *Struct. Bond.* **2006**, *119*, 89.
[58] Z. L. Hsieh, M. C. Lin, J. Y. Uan, *J. Mater. Chem.* **2011**, *21*, 1880.
[59] F. Winter, V. Koot, A. J. van Dillen, J. W. Geus, K. P. de Jong, *J. Catal.* **2005**, *236*, 91.
[60] H. Wang, X. Xiang, F. Li, *J. Mater. Chem.* **2010**, *20*, 3944.
[61] Z. Gao, J. Wang, Z. S. Li, W. L. Yang, B. Wang, M. J. Hou, Y. He, Q. Liu, T. Mann, P. P. Yang, M. L. Zhang, L. H. Liu, *Chem. Mater.* **2011**, *23*, 3509.
[62] A. L. Garcia-Ponce, V. Prevot, B. Casal, E. Ruiz-Hitzky, *New J. Chem.* **2000**, *24*, 119.
[63] D. Tichit, C. Gerardin, R. Durand, B. Coq, *Top. Catal.* **2006**, *39*, 89.
[64] F. Leroux, J. P. Besse, *Chem. Mater.* **2001**, *13*, 3507.
[65] K. Putyera, T. J. Bandosz, J. Jagiello, J. A. Schwarz, *Appl. Clay Sci.* **1995**, *10*, 177.
[66] K. Putyera, T. J. Bandosz, J. Jagieo, J. A. Schwarz, *Carbon* **1996**, *34*, 1559.
[67] T. Hibino, K. Kosuge, A. Tsunashima, *Clays Clay Miner.* **1996**, *44*, 151.
[68] F. Leroux, M. Dubois, *J. Mater. Chem.* **2006**, *16*, 4510.
[69] F. Leroux, E. Raymundo-Pinero, J. M. Nedelec, F. Beguin, *J. Mater. Chem.* **2006**, *16*, 2074.
[70] V. Prevot, E. Geraud, T. Stimpfling, J. Ghanbaja, F. Leroux, *New J. Chem.* **2010**, *35*, 169.
[71] T. Stimpfling, F. Leroux, *Chem. Mater.* **2010**, *22*, 974.
[72] Z. P. Xu, H. C. Zeng, *J. Phys. Chem. B* **2000**, *104*, 10206.
[73] Z. P. Xu, R. Xu, H. C. Zeng, *Nano Lett.* **2001**, *1*, 703.
[74] Y. D. Li, J. L. Chen, L. Chang, *Appl. Catal. A* **1997**, *163*, 45.
[75] L. Zhang, C. F. Zhang, X. Xiang, F. Li, *Chem. Eng. Technol.* **2010**, *33*, 44.

[76] Z. X. Yu, D. Chen, M. Ronning, B. Totdal, T. Vralstad, E. Ochoa-Fernandez, A. Holmen, *Appl. Catal. A* **2008**, *338*, 147.
[77] Z. X. Yu, D. Chen, B. Totdal, A. Holmen, *Mater. Chem. Phys.* **2005**, *92*, 71.
[78] Y. D. Li, J. L. Chen, L. Chang, Y. N. Qin, *J. Catal.* **1998**, *178*, 76.
[79] L. Dussault, J. C. Dupin, C. Guimon, M. Monthioux, N. Latorre, T. Ubieto, E. Romeo, C. Royo, A. Monzon, *J. Catal.* **2007**, *251*, 223.
[80] C. H. Li, Y. Zhao, K. F. Yao, J. Liang, *Carbon* **2003**, *41*, 2443.
[81] F. Li, Q. Tan, D. G. Evans, X. Duan, *Catal. Lett.* **2005**, *99*, 151.
[82] H. I. Hima, X. Xiang, L. Zhang, F. Li, *J. Mater. Chem.* **2008**, *18*, 1245.
[83] M. M. Shaijumon, N. Bejoy, S. Ramaprabhu, *Appl. Surf. Sci.* **2005**, *242*, 192.
[84] X. Xiang, L. Zhang, H. I. Hima, F. Li, D. G. Evans, *Appl. Clay Sci.* **2009**, *42*, 405.
[85] R. Benito, M. Herrero, F. M. Labajos, V. Rives, C. Royo, N. Latorre, A. Monzon, *Chem. Eng. J.* **2009**, *149*, 455.
[86] H. I. Hima, X. Xiang, L. Zhang, F. Li, D. G. Evans, *Chinese J. Inorg. Chem* **2008**, *24*, 886.
[87] Y. Zhao, Q. Z. Jiao, J. Liang, C. H. Li, *Chem. Res. Chinese U.* **2005**, *21*, 471.
[88] a) W. Y. Zhou, X. D. Bai, E. G. Wang, S. S. Xie, *Adv. Mater.* **2009**, *21*, 4565; b) Z. F. Liu, L. Y. Jiao, Y. G. Yao, X. J. Xian, J. Zhang, *Adv. Mater.* **2010**, *22*, 2285; c) Y. Li, R. L. Cui, L. Ding, Y. Liu, W. W. Zhou, Y. Zhang, Z. Jin, F. Peng, J. Liu, *Adv. Mater.* **2010**, *22*, 1508; d) J. P. Tessonnier, D. S. Su, *ChemSusChem* **2011**, *4*, 824; e) Q. Zhang, J. Q. Huang, M. Q. Zhao, W. Z. Qian, F. Wei, *ChemSusChem* **2011**, *4*, 864.
[89] Y. Zhao, Q. Z. Jiao, C. H. Li, J. Liang, *Carbon* **2007**, *45*, 2159.
[90] M. Q. Zhao, Q. Zhang, J. Q. Huang, J. Q. Nie, F. Wei, *Carbon* **2010**, *48*, 3260.
[91] Y. Cao, Y. Zhao, Q. X. Li, Q. Z. Jiao, *J. Chem. Sci.* **2009**, *121*, 225.
[92] R. L. Xue, Z. P. Sun, L. H. Su, X. G. Zhang, *Catal. Lett.* **2010**, *135*, 312.
[93] Y. Cao, Y. Zhao, Q. Z. Jiao, *Mater. Chem. Phys.* **2010**, *122*, 612.
[94] Y. Cao, Q. Z. Jiao, Y. Zhao, *Acta Phys. Chim. Sin.* **2009**, *25*, 2380.
[95] Y. Cao, Q. Z. Jiao, Y. Zhao, G. F. Song, P. Y. Zhang, *S. Afr. J. Chem.* **2010**, *63*, 58.
[96] L. Zhang, F. Li, X. Xiang, M. Wei, D. G. Evans, *Chem. Eng. J.* **2009**, *155*, 474.
[97] L. Zhang, F. Li, *Electrochim. Acta* **2010**, *55*, 6695.
[98] Q. Zhang, M. Q. Zhao, D. M. Tang, F. Li, J. Q. Huang, B. L. Liu, W. C. Zhu, Y. H. Zhang, F. Wei, *Angew. Chem. Int. Ed.* **2010**, *49*, 3642.
[99] M. Q. Zhao, J. Q. Huang, Q. A. Zhang, J. Q. Nie, F. Wei, *Carbon* **2011**, *49*, 2148.
[100] D. S. Su, *Angew. Chem. Int. Ed.* **2011**, *50*, 4747.
[101] a) Q. Zhang, M. Q. Zhao, J. Q. Huang, Y. Liu, Y. Wang, W. Z. Qian, F. Wei, *Carbon* **2009**, *47*, 2600; b) Q. Zhang, M. Q. Zhao, J. Q. Huang, J. Q. Nie, F. Wei, *Carbon* **2010**, *48*, 1196.
[102] D. Gournis, M. A. Karakassides, T. Bakas, N. Boukos, D. Petridis, *Carbon* **2002**, *40*, 2641.
[103] a) R. Fernandez-Saavedra, P. Aranda, E. Ruiz-Hitzky, *Adv. Funct. Mater.* **2004**, *14*, 77; b) A. Gomez-Aviles, M. Darder, P. Aranda, E. Ruiz-Hitzky, *Appl. Clay Sci.* **2010**, *47*, 203; c) J. Q. Nie, Q. Zhang, M. Q. Zhao, J. Q. Huang, Q. A. Wen, Y. Cui, W. Z. Qian, F. Wei, *Carbon* **2011**, *49*, 1568; d) E. Ruiz-Hitzky, M. Darder, F. M. Fernandez, E. Zatile, F. J. Palomares, P. Aranda, *Adv. Mater.* **2011**, *23*, 5250.
[104] M. Q. Zhao, Q. Zhang, J. Q. Huang, J. Q. Nie, F. Wei, *ChemSusChem* **2010**, *3*, 453.
[105] a) Q. Zhang, J. Q. Huang, M. Q. Zhao, W. Z. Qian, Y. Wang, F. Wei, *Carbon* **2008**, *46*, 1152; b) D. L. He, M. Bozlar, M. Genestoux, J. B. Bai, *Carbon* **2010**, *48*, 1159; c) M. Bozlar, D. L. He, J. B. Bai, Y. Chalopin, N. Mingo, S. Volz, *Adv. Mater.* **2010**, *22*, 1654; d) D. Y. Kim, H. Sugime, K. Hesegawa, T. Osawa, S. Noda, *Carbon* **2011**, *49*, 1972.
[106] a) D. S. Su, R. Schlogl, *ChemSusChem* **2010**, *3*, 136; b) Y. Q. Sun, Q. O. Wu, G. Q. Shi, *Energy Environ. Sci.* **2011**, *4*, 1113.
[107] a) E. Frackowiak, F. Beguin, *Carbon* **2001**, *39*, 937; b) L. L. Zhang, X. S. Zhao, *Chem. Soc. Rev.* **2009**, *38*, 2520; c) A. G. Pandolfo, A. F. Hollenkamp, *J. Power Sources* **2006**, *157*, 11.
[108] a) H. Jiang, T. Zhao, C. Z. Li, J. Ma, *J. Mater. Chem.* **2011**, *21*, 3818; b) T. Zhao, H. Jiang, J. Ma, *J. Power Sources* **2011**, *196*, 860.
[109] a) T. R. Jow, J. P. Zheng, *J. Electrochem. Soc.* **1998**, *145*, 49; b) M. Toupin, T. Brousse, D. Belanger, *Chem. Mater.* **2002**, *14*, 3946.
[110] M. Mastragostino, C. Arbizzani, F. Soavi, *Solid State Ionics* **2002**, *148*, 493.
[111] A. Malak-Polaczyk, C. Vix-Guterl, E. Frackowiak, *Energ. Fuel.* **2010**, *24*, 3346.
[112] R. Ma, K. Takada, K. Fukuda, N. Iyi, Y. Bando, T. Sasaki, *Angew. Chem. Int. Ed.* **2008**, *47*, 86.
[113] a) C. Liu, F. Li, L.-P. Ma, H.-M. Cheng, *Adv. Mater.* **2010**, *22*, E28; b) H. Li, Z. Wang, L. Chen, X. Huang, *Adv. Mater.* **2009**, *21*, 4593.
[114] J. R. Dahn, T. Zheng, Y. Liu, J. S. Xue, *Science* **1995**, *270*, 590.
[115] L. Ji, Z. Lin, M. Alcoutlabi, X. Zhang, *Energy Environ Sci* **2011**, *4*, 2682.
[116] M. Latorre-Sanchez, P. Atienzar, G. Abellan, M. Puche, V. Fornes, A. Ribera, H. García, *Carbon* **2012**, *50*518
[117] J. N. Coleman, U. Khan, W. J. Blau, Y. K. Gun'ko, *Carbon* **2006**, *44*, 1624.
[118] L. Liu, J. C. Grunlan, *Adv. Funct. Mater.* **2007**, *17*, 2343; D. Sun, C. C. Chu, H. J. Sue, *Chem. Mater.* **2010**, *22*, 3773.
[119] F. Li, X. Duan, *Struct. Bond.* **2006**, *119*, 193.
[120] X. C. Gui, J. Q. Wei, K. L. Wang, A. Y. Cao, H. W. Zhu, Y. Jia, Q. K. Shu, D. H. Wu, *Adv. Mater.* **2010**, *22*, 617.
[121] Z. J. Fan, J. Yan, G. Q. Ning, T. Wei, W. Z. Qian, S. J. Zhang, C. Zheng, Q. Zhang, F. Wei, *Carbon* **2010**, *48*, 4197.
[122] A. Y. Cao, P. L. Dickrell, W. G. Sawyer, M. N. Ghasemi-Nejhad, P. M. Ajayan, *Science* **2005**, *310*, 1307.
[123] a) G. P. Rao, C. Lu, F. Su, *Sep. Purif. Technol.* **2007**, *58*, 224; b) A. V. Bazhenov, T. N. Fursova, S. S. Grazhulene, A. N. Red'kin, G. F. Telegin, *Fullerenes, Nanotubes, Carbon Nanostruct.* **2010**, *18*, 564.
[124] a) S. Miyata, *Clays Clay Miner.* **1983**, *31*, 305; b) P. K. Dutta, M. Puri, *J. Phys. Chem.* **1989**, *93*, 376.
[125] a) R. L. Goswamee, P. Sengupta, K. G. Bhattacharyya, D. K. Dutta, *Appl. Clay Sci.* **1998**, *13*, 21; b) N. N. Das, J. Konar, M. K. Mohanta, S. C. Srivastava, *J. Colloid Interface Sci.* **2004**, *270*, 1.
[126] N. K. Lazaridis, *Water Air Soil Pollut.* **2003**, *146*, 127.
[127] a) M. Jakupca, P. K. Dutta, *Chem. Mater.* **1995**, *7*, 989; b) P. K. Dutta, D. S. Robins, *Langmuir* **1994**, *10*, 1851.
[128]a) S. K. Vashist, D. Zheng, G. Pastorin, K. Al-Rubeaan, J. H. T. Luong, F. S. Sheu, *Carbon* **2011**, *49*, 4077; b) Z. Liu, S. Tabakman, K. Welsher, H. J. Dai, *Nano Res.* **2009**, *2*, 85.
[129] X. M. Sun, Z. Liu, K. Welsher, J. T. Robinson, A. Goodwin, S. Zaric, H. J. Dai, *Nano Res.* **2008**, *1*, 203.
[130] H. Jin, D. A. Heller, M. S. Strano, *Nano Lett.* **2008**, *8*, 1577.
[131] K. Kostarelos, L. Lacerda, G. Pastorin, W. Wu, S. Wieckowski, J. Luangsivilay, S. Godefroy, D. Pantarotto, J. P. Briand, S. Muller, M. Prato, A. Bianco, *Nat. Nanotechnol.* **2007**, *2*, 108.
[132] E. Heister, V. Neves, C. Tilmaciu, K. Lipert, V. S. Beltran, H. M. Coley, S. R. P. Silva, J. McFadden, *Carbon* **2009**, *47*, 2152.
[133] a) Z. P. Xu, G. Q. Lu, *Pure Appl. Chem.* **2006**, *78*, 1771; b) Y. Li, D. Liu, H. H. Ai, Q. Chang, D. D. Liu, Y. Xia, S. W. Liu, N. F. Peng, Z. G. Xi, X. Yang, *Nanotechnology* **2010**, *21*, 105101.
[134] a) J. M. Oh, S. J. Choi, G. E. Lee, S. H. Han, J. H. Choy, *Adv. Funct. Mater.* **2009**, *19*, 1617; b) J. H. Choy, J. S. Jung, J. M. Oh, M. Park, J. Jeong, Y. K. Kang, O. J. Han, *Biomaterials* **2004**, *25*, 3059; c) J. H. Choy, S. J. Choi, J. M. Oh, T. Park, *Appl. Clay Sci.* **2007**, *36*, 122.